A global database of accreted Ocean Plate Stratigraphy (OPS): towards reconstructing subducted hotspot tracks.

Ikhwan Rasyidin Hadi Abbas

M.Sc Student of Graduate School of Geoscience, Utrecht University

Abstract

This thesis presents a comprehensive exploration of Mesozoic Oceanic Plate Stratigraphy (OPS) within accreted orogenic belts, with a specific focus on identifying and compiling Mid-Ocean Ridge Basalts (MORB) and Ocean Island Basalts (OIB) to reconstruct subducted hotspot tracks. The study encompasses diverse geological locales, especially in the Circum Pacific, including Japan, Russia, the Philippines, Costa Rica, Mexico, California, Alaska, and New Zealand, leveraging extensive geological data to unravel the historical trajectory of ancient Pacific Plates. The research primarily centers on elucidating the geological history of ancient oceanic remnants associated with the Izanagi Plate, Farallon Plates, and Phoenix Plates, emphasizing the geochemical affinity of the volcanic features and the ages of oceanic floor and seamount birth. The study reveals that ocean floor and seamounts accreted from the Late Carboniferous to the Late Cretaceous in various geological timeframes. A key contribution of this research lies in refining the early formation of the Pacific Plate, drawing on geochronological affinity and volcanic feature ages within the OPS Sequence. These findings offer a nuanced perspective, potentially revising previous estimations and enriching our comprehension of early plate tectonics.

Furthermore, the study identifies a slight predominance of Mesozoic hotspot distribution in the southern hemisphere, aligning with the contemporary configuration of the Pacific Plate. The research underscores the importance of further analyses, including dating ages, paleomagnetic studies, and geochemical assessments of selected volcanic features. These endeavors are pivotal in advancing our understanding of plate tectonics and the evolution of the Pacific Plate, ultimately contributing to a more accurate portrayal of Earth's dynamic geological history.

Abstrak

Tesis ini menyajikan eksplorasi komprehensif mengenai Stratigrafi Lempeng Samudera Mesozoik (OPS) dalam sabuk orogenik yang terakresi, dengan fokus khusus pada identifikasi dan kompilasi *Mid-Ocean Ridge Basalts* (MORB) dan *Ocean Island Basalts* (OIB) untuk merekonstruksi jejak hotspot yang tersubduksi. Studi ini mencakup berbagai lokasi geologis terutama di sekitar Pasifik, termasuk Jepang, Rusia, Filipina, Kosta Rika, Meksiko, California, Alaska, dan Selandia Baru, dengan memanfaatkan data geologi yang luas untuk mengungkapkan lintasan sejarah Lempeng Pasifik purba. Penelitian ini terutama berfokus pada mengungkap sejarah geologis sisa-sisa dari lantai samudera purba yang terkait dengan Lempeng Izanagi, Lempeng Farallon, dan Lempeng Phoenix, dengan menekankan afinitas geokimia dari batuan vulkanik dan usia awal kemunculan lantai samudera serta gunung api bawah laut. Studi ini menemukan bahwa pemekaran lantai samudera dan pembentukan gunung laut diketahui sudah terjadi sejak zaman Karbon Akhir terus berlangsung hingga Kapur Akhir yang kemudian lantai samudra dan gunung api bawah laut ini terakresikan dalam berbagai rentang waktu geologis. Setidaknya terdapat 28 lokasi yang memiliki afinitas magma OIB dan 30 lokasi yang menunjukkan pemekaran lantai samudra (MORB). Kontribusi utama dari penelitian ini terletak pada investigasi pembentukan awal Lempeng Pasifik, dengan mengandalkan afinitas geokronologis dan umur batuan vulkanik and umur turbidit sediment dalam urutan OPS. Temuan ini menawarkan perspektif yang halus, berpotensi memperkaya pemahaman kita tentang awal mula tektonik lempeng dan pemekaran Lantai Pacifik.

Selain itu, studi ini mengidentifikasi sedikit dominannya distribusi hotspot pada Mesozoikum di belahan bumi selatan dibandingkan dengan belahan bumi utara, sejalan dengan konfigurasi kontemporer dari Lempeng Pasifik. Penelitian ini menekankan pentingnya analisis lebih lanjut, termasuk penanggalan usia, studi paleomagnetik, dan penilaian geo-kimia pada fitur vulkanik tertentu. Upaya-upaya ini sangat penting dalam memajukan pemahaman kita tentang tektonik lempeng dan evolusi Lempeng Pasifik, akhirnya berkontribusi pada gambaran yang lebih akurat tentang sejarah geologis dinamis Bumi.

Introduction

The dynamic evolution of the Earth's surface is a testament to the intricate interplay of global tectonic forces. Our understanding of this complex geological narrative has been enriched through the analysis of petrological, geochemical, dating, and paleomagnetic data, which collectively reveal the commencement of Earth's plate motion (subduction) during the Neoproterozoic era (Condie et al., 2006; Stern, 2007). Subduction processes have been crucial in reshaping the Earth's lithosphere throughout geological time, recycling nearly 60 percent of it in the last 150 million years (Torsvik et al., 2010), and about 93 percent has been recycled since 2.5 Ga ago (Hawkesworth et al., 2010). These ancient geological processes have left behind intriguing remnants, often nestled within accretionary belts, which provide the only evidence for reconstructing the paleographic of the lost oceans (Cawood & Buchan, 2007), particularly through the paleogeographic reconstruction of accreted Ocean Plate Stratigraphy (OPS) (Isozaki et al., 1990; Wakita & Metcalfe, 2005; Kusky et al., 2013; Boschman et al., 2018, 2019, 2021; van Hinsbergen et al., 2020; van Hinsbergen & Schouten, 2021).

Recent research endeavors have unveiled an intriguing asymmetry in the distribution of oceanic hotspots across the Earth's hemispheres. As reported by (Jackson et al. (2021) and Jackson & Macdonald (2022), the southern hemisphere show boasts twice as many of these enigmatic features compared to its northern counterpart (Figure 1). This revelation not only prompts questions about the contemporary Earth but also beckons us to explore its historical counterpart. Has this asymmetry manifested in the past? To address this fundamental question, here we present volcanic features (basaltic rocks) related to a mid-oceanic ridge (MOR) and/or ocean island (OI) types within the OPS sequence, with a particular focus on the Late paleozoic to Mesozoic periods. By scrutinizing the distribution of seamounts during this epoch, we endeavor to unravel the historical underpinnings of this intriguing phenomenon.

The cornerstone of our research lies in establishing a comprehensive and globally accessible database of accreted Ocean Plate Stratigraphy (OPS) within pacific plates. This database aims to serve as a foundational resource, enabling the meticulous tracing of hotspot and seamount locations during the Mesozoic era and the ancient pacific thetys.

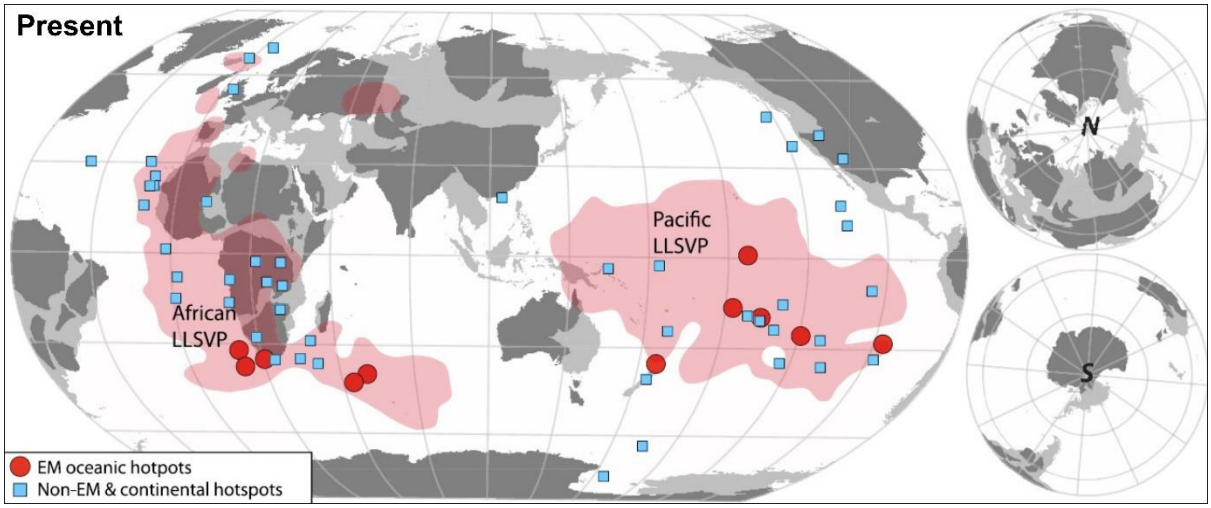

Figure 1. The 11 oceanic EM hotspot conduit locations are shown as large red circles, while the continental and non-EM oceanic hotspot conduit locations are shown as smaller blue squares (Jackson & Macdonald, 2022)

Definition of Ocean Plate Stratigraphy

The stratigraphy of the Oceanic Plate was first defined by (Isozaki et al., 1990) as 'Ocean Plate Stratigraphy or OPS'. The oceanic plate stratigraphy is an idealized stratigraphic succession of the seafloor, reconstructed from mixtures of ancient protoliths or accretionary complexes. It is generally reconstructed by biostratigraphy of radiolaria, conodont, and fusulinid microfossils (Wakita & Metcalfe, 2005). Radiolarians are the most useful because they occur throughout the Phanerozoic and in various lithologies, argillaceous, siliceous, or calcareous.

The ideal stratigraphic column is depicted in Figure 2. It shows that the protolith of a Paleozoic to Mesozoic accretionary complex in Japan has been used to reconstruct the stratigraphy of oceanic plates (Isozaki et al., 1990; Wakita & Metcalfe, 2005). OPS commonly comprises pillow basalt, chert, ± limestone, ± siliceous shale and detrital turbidite in ascending order (Isozaki et al., 1990; Wakita & Metcalfe, 2005). A recommended OPS sequence begins with pillow basalt and then moves upwards via radiolarian chert, limestone, siliceous shale, shale, and sandstone. Compared to detrital clastic rocks, the period covered by chert is substantially wider. However, because detrital sediments have a higher sedimentation rate than pelagic chert, the clastic component of OPS that originates from detritus is thicker (Isozaki et al., 1990; Wakita & Metcalfe, 2005).

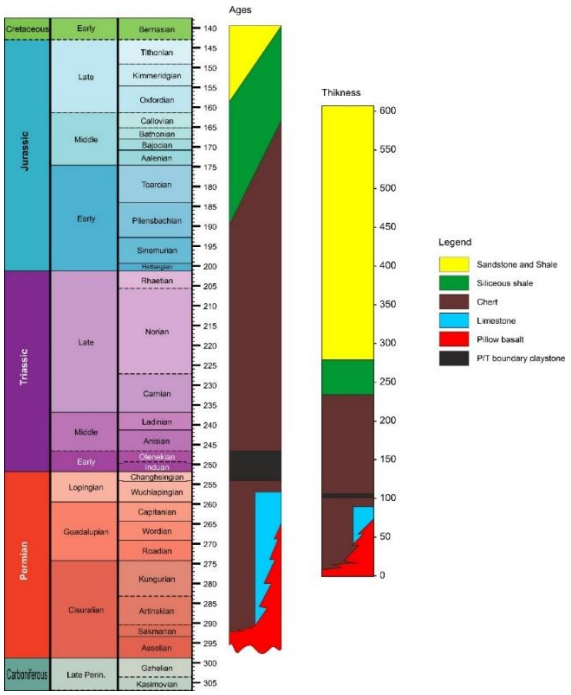

Figure 2. An ideal oceanic plate stratigraphy (OPS) sequence. The illustration was reconstructed from a Jurassic accretionary complex in Japan. It shows pillow basalt, chert, limestone, siliceous shale, sandstone, and shale in ascending order. Moified from Wakita & Metcalfe (2005)

The pillow basalts in the OPS sequence have an alkaline-basalt chemical composition indicating as seamount or ridge-origin, – which at some locations, such as Japan ACs, is overlain by reefal limestones – depends on the carbonate composition depth, and transition into reef detritus, commonly observed on the flanks of seamounts or the surrounding oceanic floor (H. Sano, 1988a, 1988b; Okamura, 1991). The siliceous skeletons of radiolarians, deposited as "marine snow" on the ocean floor, undergo diagenesis and transform into chert over time. On or near the seamount flanks are alternating layers of calcareous detrital pieces and siliceous radiolarian oozes, leading to interbedded limestones and chert forming. The chert deposit, known as 'bedded' or 'ribbon-bedded' chert, exhibits a layered structure with thin shale layers interleaved with overlying radiolarian chert. These ribbon-bedded chert's age ranges and thicknesses provide insights into the extremely slow sedimentation rate. Importantly, these cherts lack any detrital fragments originating from continental sources. The slow sedimentation rate and absence of continental fragments suggest that ribbon-bedded radiolarian cherts were formed as pelagic sediments on the ocean floor. The age range of chert in an OPS sequence indicates the age and duration of the ocean floor, from its origin at the mid-ocean ridge to its end at the trench (Isozaki et al., 1990; Wakita & Metcalfe, 2005). Oceanic radiolarian chert transitions upwards into siliceous shale, predominantly composed of fine-grained debris and radiolarian remains. More radiolarians and a slower sedimentation rate than usual detrital deposits point to a hemipelagic environment near the continental edge on the trench's offshore side. The siliceous shale is succeeded by shale interbedded with thin sandstone strata, followed by a turbidite sequence dominated by sandstone. The younger turbidite sequence contains enormous coarse-grained sandstones close to the surface. The shale-dominated and

sandstone-dominated sequences are flysch-type sedimentary rocks deposited near or within the trench by turbidity currents.

Figure 3 shows the Ocean Plate Stratigraphy successions document the geologic evolution of the ocean floor, from its birth at the mid-ocean ridge to its end at the subduction zone at the convergent plate margin. The formation of volcanic islands near shallow oceanic ridges, followed by the deposition of reef limestone as the oceanic plate moved away from the ridge and subsided, explains the presence of basalt beneath the reef limestone in the lower part of the succession. Another possibility is volcanic islands formed through within-plate volcanism associated with basalt and reef limestone hotspots, such as the Hawaiian-Emperor Chain. The geochemical characteristics of the basalts can help differentiate between these two scenarios. The interbedding of limestone and chert indicates a rock facies that forms in the ocean, typically near or on the flanks of volcanic islands or seamounts, likely around the carbonate compensation depth (CCD). Ribbon-bedded radiolarian chert, formed from radiolarian ooze deposited beneath the CCD on the ocean floor, provides a record of the plate's journey from the subsided volcanic islands or seamounts to its arrival at the subduction trench along the continental margin. Before the oceanic plate reached the trench, siliceous muds and radiolarian cherts were deposited in the hemipelagic region. Upon reaching the trench, the segment of the oceanic plate covered by radiolarian chert and siliceous clay is subsequently overlain by flysch-type trench-fill sediments.

Within the accretionary wedge, the upper sections of the Ocean Plate Stratigraphy (OPS) are removed through tectonic scraping and are subsequently layered within the accretionary prism. On the other hand, the lower portions of the OPS are incorporated into the accretionary prism through underplating, where they are thrust beneath the overriding plate. The accreted volcanic islands, known as seamounts, undergo erosion along deep-seated decollement faults. As a result, these accreted sediments undergo multiple deformation and disruption processes.

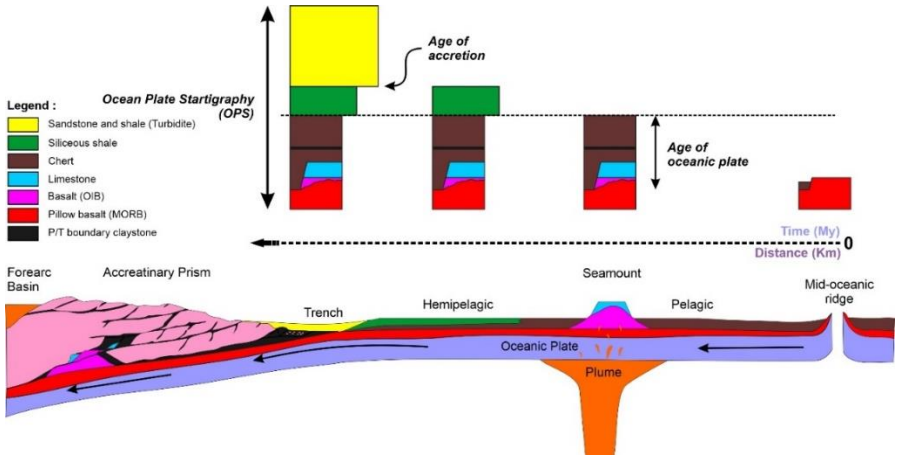

Figure 3. The sketch shows an oceanic plate's travelogue from its origin at the mid-oceanic ridge to its subduction at the trench to illustrate the concept of ocean plate stratigraphy (OPS). Modified from Isozaki et al., (1990) and Wakita & Metcalfe, (2005)

Geology Setting

The Panthalassa Ocean, which surrounded the Pangea supercontinent during the late Paleozoic-early Mesozoic era, contained multiple tectonic plates that have undergone subduction over time. As the Pangea supercontinent began to break apart, landmasses separated, and the Panthalassa Ocean shrunk. Eventually, the Panthalassa Ocean transformed into the Pacific Ocean as the movement of tectonic plates continued. Through the analysis of marine magnetic anomalies, it has been determined that the Panthalassa Ocean once hosted three significant oceanic plates: Farallon, Phoenix, and Izanagi. The Pacific Plate, which now underlies the Pacific Ocean, formed around 190 million years ago at a triple junction involving these plates and grew as a result of subduction and the eventual disappearance of the Farallon, Phoenix, and Izanagi plates (Larson & Chase, 1972; Larson & Pitman, 1972; Boschman & van Hinsbergen, 2016). This transformation is reflected in the Pacific triangle, an area in the western Pacific where three Mesozoic magnetic lineation sets intersect (Japanese, Hawaiian, and Phoenix lineations), marking the birth of the Pacific plate from its three precursor plates (Seton et al., 2012; Müller & Seton, 2015; Boschman & van Hinsbergen, 2016; Boschman et al., 2021). These precursor plates separated into the eastern, southern, and western regions of Panthalassa (Figure 4).

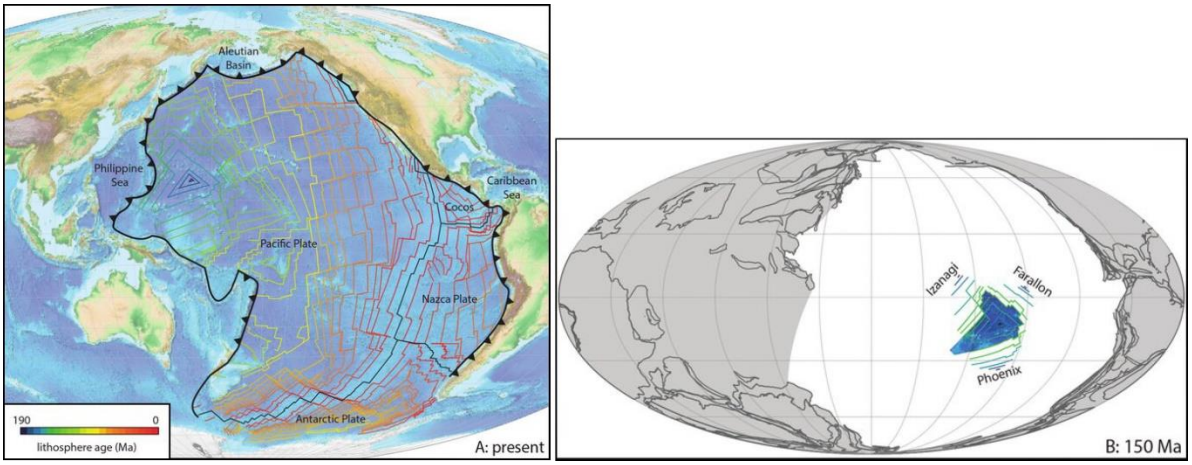

Figure 4. (A) Modern Pacific Ocean plate configuration and isochrons (B) Latest Jurassic Panthalassa Ocean, including the young and growing Pacific Plate (in blue) and its conjugates, the Farallon, Izanagi, and Phoenix plates (Boschman et al., 2021)

The remnants of the Farallon plates of the eastern Phantalassa ocean are expected to be found in the accretionary complex in North and Central America: in Alaska (Chugach Terrane), California (Franciscan Complex), in Mexico (Cedros Island and Vizcaino Peninsula) and Costa Rica (Santa Elena Peninsula) (Connelly et al., 1977; Connelly, 1978; Kusky et al., 1997, 2013; Kimbrough & Moore, 2003; Baumgartner & Denyer, 2006; Centeno-García et al., 2008; Wakabayashi, 2017; Boschman et al., 2018, 2019). However, the remnant of the Farallon plate may not be present in South America due to the South American margin experiencing subduction erosion rather than accretion during the Mesozoic-Cenozoic (Kennan & Pindell, 2009; Pindell & Kennan, 2009; Escalona et al., 2021) except for accreted oceanic fragments in the northernmost Andes of Colombia and Ecuador related to Late

Cretaceous collision with the Caribbean Plate (Kennan & Pindell, 2009; Horton, 2018; Montes et al., 2019).

The remnants of the Phoenix Plate are expected to be found along the continental margins of the southern Panthalassa Ocean, including areas in Antarctica, New Zealand, Australia, and Southeast Asia. The accreted relics of the Phoenix Plate can be observed in Southeast Asia (for example, Jasin & Tongkul, 2013). However, interpreting these records is challenging due to intense deformation in the region where the Tethyan and Panthalassa plate systems intersect (e.g., Boschman & van Hinsbergen, 2016; Boschman et al., 2021). The remnants of the Phoenix Plate are believed to have accreted at former Gondwana margins. In New Zealand's North Island, specific examples of accreted relics from the Phoenix Plate can be found. For instance, OPS is exposed in the Waipapa Terrane, a northwest-southeast trending accretionary complex belt (e.g., Aita & Spörli, 1992; Black, 1994; Takemura et al., 2002). Other areas in New Zealand, such as the Torlesse Terrane and Otago Schist Complex, also provide evidence of accreted relics from the Phoenix Plate (e.g. P. M. Barnes & Korsch, 1991; Wandres & Bradshaw, 2005; Wandres et al., 2005; Fagereng & Cooper, 2010).

The remnants of western Phantalassa (Izanagi Plate) are well preserved in the Japanese islands and contain a ~500 Ma record of accretionary orogenesis related to the long-lived subduction of Panthalassa lithosphere (Maruyama & Seno, 1986; Isozaki, 1996) – first along the continental margin of the China blocks (part of Eurasia since the mid-Mesozoic), and since Oligocene – Miocene opening of the Sea of Japan, at the Japanese island arc (Isozaki, 1996, 2000; Maruyama et al., 1997a; Isozaki et al., 2010). The long-lived subduction led to two accretionary complexes growing younger toward a trench. These complexes are divided by the Median Tectonic Line (MTL) (Isozaki et al., 1990; Isozaki, 2000), a significant fault running east to west and dipping northward. Currently, the MTL is experiencing a right-lateral strike-slip movement at a rate of approximately 5 to 10 millimeters per year. This motion is seen as a result of strain partitioning in the overriding plate due to the oblique subduction occurring at the Nankai Trough (Okada, 1973; Sugiyama, 1994). The MTL juxtaposes an outer accretionary region in the south with an inner accretionary region in the north. The presence of similar fauna in the inner zone and South Primorye (Far East Russia) suggests that by the Permian period, the inner zone had already been positioned adjacent to the Asian continent before the opening of the Sea of Japan (I. Hayami, 1961; T. Sato, 1962; Kobayashi & Tamura, 1984a; Tazawa, 2002).

In contrast, the outer zone contains a wide range of Triassic to Jurassic faunal communities with characteristics more aligned with the Tethyan region (Matsumoto, 1978; Kobayashi & Tamura, 1984a; L. Hayami, 1984; Hallam, 1986). Sediment provenance studies have revealed a connection between the Lower Cretaceous sedimentary rocks in the outer zone and the South China Block (Ikeda et al., 2016); during the Late Cretaceous, there was the development of a left-lateral pull-apart basin along the MTL (the Izumi Group) (Ichikawa et al., 1979, 1981; Kobayashi & Tamura, 1984b; Miyata, 1990; Noda & Toshimitsu, 2009; Noda & Sato, 2018). Several authors have proposed a tectonic model in which the

MTL accommodated large (1000 km) left-lateral margin parallel strike-slip motion, bringing the outer zone from a low-latitude position to its modern position juxtaposed against the inner zone during the Cretaceous (Taira et al., 1983; Yamakita & Otoh, 2000; Yao, 2000; Sakashima et al., 2003). However, a klippe of inner zone units overlying the outer zone has been identified. Geophysical data show that the accretionary complexes of the outer zone are buried below the inner zone orogen far beyond the surface transect of the MTL, which has led others to argue that the inner and outer zones were juxtaposed by thrusting (Isozaki, 1988b; Isozaki & Itaya, 1991; H. Sato et al., 2005, 2015; T. Ito et al., 2009). Boschman et al. (2019 and 2021) have proposed a tectonic reconstruction indicating that in the mid-Cretaceous period, the outer zone was likely separated from the Northeast Asian continental margin by a back-arc basin. According to Boschman et al. (2021), the outer zone rifted away from the South China Block during the Jurassic, underwent ongoing accretion in the Jurassic-Cretaceous period within an interoceanic setting, and eventually accreted to the inner zone orogen in the Late Cretaceous. (Boschman et al., 2021) illustrated through a reconstruction of intra-oceanic subduction at the Oku-Niikappu arc that in mid-Cretaceous time, the outer zone was likely separated from the Northeast Asian continental margin by a back-arc basin. We follow its tectonic reconstruction in which the outer zone orogen rifted off the South China Block in the Jurassic, experienced ongoing accretion in Jurassic-Cretaceous time in an intraoceanic position, and accreted to the inner zone orogen in the Late Cretaceous. The pre-Middle Jurassic position of the outer zone follows the tectonic reconstructions of Ikeda et al. (2016), Uno et al. (2011), Sakashima et al. (2003), and Tazawa (2002).

Result

Upper Paleozoic – Mesozoic Circum-Pacific OPS

Based on our database (appendix Table 1), the accreted OPS dating from the late Paleozoic to the Mesozoic era within the circum-Pacific region is observed in various locations, including Russia (specifically in the Sakhalin Island), Japan, the Philippines, New Zealand, Costa Rica, Mexico, California, and Alaska, as illustrated in Figure 5. The distribution of late Paleozoic basaltic rocks (depicted in red and dark blue points in Figure 5) from the Mesozoic Arc Complexes (ACs) is extensively documented in Japan compared to other regions. Meanwhile, the distribution of basaltic rocks from the Mesozoic era (indicated in green, light blue, and purple points in Figure 5) is well-documented in nearly all of these regions except South America.

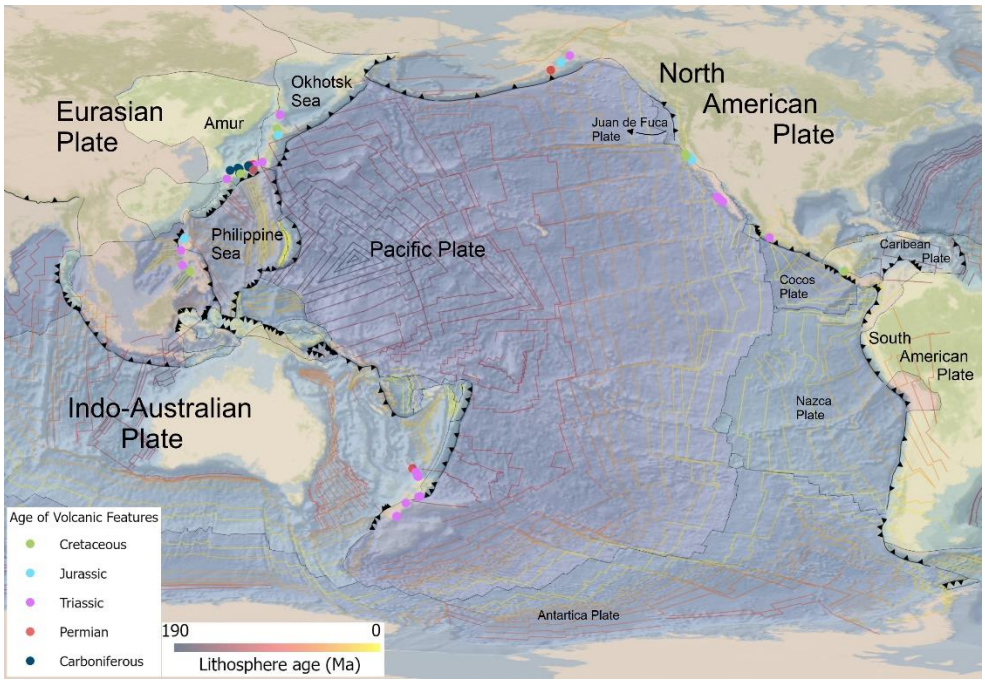

Figure 5. Distribution of the volcanic rocks from the OPS sequence in Circum Pacific (Isochrons line from Seton et al. (2020).

- **Russia**

The Susunai Complex on Sakhalin Island, Russia, hosts the Shakalin Island OPS (Rikhter, 1981; Kimura et al., 1992; Zharov, 2005). The Susunai Complex is considered the northern extension of the Kamuikotan Metamorphic Belt in Hokkaido, Japan, and is part of the circum-Pacific blueschist belts. It is between Cretaceous fore-arc sediments and the relatively shallow Cretaceous Aniva Accretionary Complex (Kimura et al., 1992). The Susunai Complex primarily consists of metamorphosed basalt, which displays features of original pillow lava, pillow breccia, hyaloclastite, reworked basaltic sediments, amphibolites, metacherts, metagreywacke, and metapelites (Kimura et al., 1992). In certain areas, such as Socole and the Kamisarovoka River, the complex also includes serpentinite melange along its northern and southern margins (Rikhter, 1981). The radiometric age of K-Ar and Zircon track

dating the Susunai Complex ranges from 220 to 55 million years, with three prominent peaks at 178-206 Ma, 133-148 Ma, and 55-77 Ma (Yegorov, 1967; Dobretsov & Kuroda, 1969; Khanchuk et al., 1988; Zharov, 2005) and Shakalin turbidite (61.9–59.7 Ma, using K-Ar and Rb-Sr dating) (Zharov, 2005)

The OPS sequence of the Susunai Complex, located on South Sakhalin Island and facing the Okhotsk Sea coastline in Ostry Cape, has been documented by Kimura et al. (1992). It exhibits a domal structure, as reported by (Rikhter, 1981). The sequence alternates between greenschist facies rocks, including pillow basalts, pillow breccias, hyaloclastite, reworked basaltic volcaniclastic deposits, and metachert and pelitic schist. Basaltic rock is associated with pelagic limestones found in Anna River, as Kimura et al. (1992) reported. The basaltic rocks within this sequence exhibit characteristics similar to mid-ocean ridge basalts (MORB), except for a sample from Anna River, which shows characteristics of seamount-type basalt. The ages K-Ar dating of these rocks range from 206 Ma, 177-179 Ma (Zharov, 2005).

Paleomagnetic of the Late Cretaceous of the brown-red siltstones (Campanian-Maastichian; 75 ± 9 Ma) (Bazhenov et al., 2001), the South Sakhalin show inclination between -53.3° and 75.6° and paleolatitude 26.6 ± 5.2° N (Bazhenov et al., 2001) – detailed in Appendix Table 2.

- **Japan**

Accretionary complexes hosting OPS formations in Japan formed in the Paleo-Pacific Ocean, during a long period from the Carboniferous until the Cretaceous (e.g. (Isozaki et al., 1990, 2010; Isozaki, 1997; Maruyama et al., 1997b; Safonova et al., 2009, 2016; Kusky et al., 2013; Safonova & Santosh, 2014; Safonova, Kojima, et al., 2015). These OPS found in Japan on the Honshu, Kyushu, Shikoku, and Hokkaido islands occur in the Akiyoshi, Mino–Tamba–Ashio, Chichibu, Sorachi-Yezo and Northern Shimanto ACs. The OPS formations of these ACs were accreted to the active margin of East Asia, respectively, during the Late Permian, Middle-Late Jurassic, and Late Cretaceous (e.g., Taira et al., 1982; H. Sano, 1988a, 1988b; H. Sano & Kanmera, 1988; Isozaki et al., 1990; Onoue et al., 2004; Wakita, 2012)

Akiyoshi OPS is an accretionary complex hosting Carboniferous–Permian OPS units occurs in the Omi, Atetsu, Taishaku, Akiyoshi and Hirao areas in SW Japan and consists of three fault-bounded units: carbonate (unit A), siliceous–terrigenous (Unit B) and carbonate–terrigenous (unit C) (Figure 6) (Kanmera & Sano, 1991; Nakashima & Sano, 2007; Safonova, Kojima, et al., 2015; Safonova et al., 2016). The OPS sequence in these ACs varied from basalt-carbonate-silicic tuff, basalt-chert-silicic tuff covered by sandstone (filling trench turbidite).

According to some researchers, the carbonate and chert (spiculite and radiolarian), through the analysis of various fossils and microfossils, have age range from the Early Carboniferous (Visean) to the late Middle Permian (Capitanian) (Kanmera et al., 1990; Isozaki, 1997; H. Sano, 2006). Both carbonate and chert sequences are covered by basalt-volcaniclastic rocks (Kanmera & Sano, 1991). The

covered sandstone as the filling trench turbidite, dominated by siliceous mudstone and siliciclastic sandstone derived from terrestrial sources, overlies the chert layers and is estimated to date back to the earliest Late Permian (H. Sano et al., 1987).

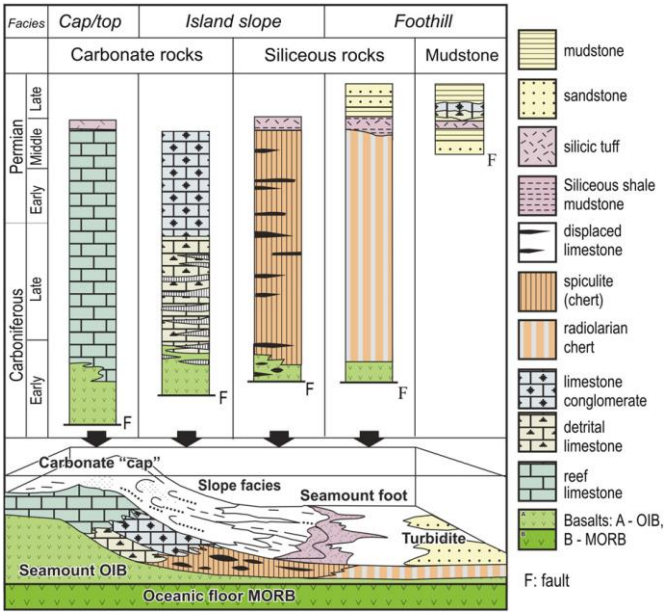

Figure 6. A seamount OPS reconstructed from the Akiyoshi accretionary complex showing several facies of an oceanic island: carbonate "cap", carbonate-volcanogenic slope facies breccia and clastics, basal mudstone-shale and chert (From Kanmera & Sano, 1991). When approaching the trench, the OPS rocks get covered by mudstone–sandstone turbidites.

The Akiyoshi OPS, as detailed in Safonova et al. (2015, 2016), is characterized by volcanic features and is distributed across Akiyoshi-dai (Edo, Yamaguchi), Taishaku-dai (Kochi), and Atetsu-dai (Kochi). In the Yamaguchi Prefecture, one of the locations of the OPS sequence in the Akiyoshi OPS is near Edo Village. Basaltic rocks in this area are found to be overlain by massive limestone, as reported by Safonova et al. (2016) and Safonova et al. (2015). Kanmera and Sano (1991) and Sano (2006) describe the basalt unit within the Akiyoshi-dai OPS sequence as primarily comprising basaltic volcaniclastic rocks, with minor occurrences of pillow lavas. The lavas and volcanic breccias in the area exhibit high vesicularity. Moreover, the basaltic rocks within the Akiyoshi terrane have undergone greenschist facies metamorphism, as Safonova et al. (2015) stated. According to Sano (2006), the mafic volcanic rocks, predominantly basalts, within the Akiyoshi AC are commonly associated with Visean (Lower Carboniferous) to Middle Permian carbonates. Additionally, a geochemical study conducted by (Maruyama et al., 1997b) reveals that the basaltic rocks from the Akiyoshi OPS represent Oceanic Island Basalts (OIBs).

The Mino-Tamba-Ashio ACs, which occupy a large part of Japan, comprise accreted sedimentary and magmatic rocks of Carboniferous to Jurassic age OPS. The OPS sequence is dominated by Carboniferous–Permian basalts and limestone and Permian–Jurassic chert (H. Sano & Kojima, 2000; Nakae, 2000). First, Sano and Kojima (2000) argued that the Mino-Tamba Permian limestones originated on the cap of an oceanic seamount based on geological data. It was later proven by the

occurrences beneath the OIB-type basalts (S. Sano et al., 2000; Safonova, Kojima, et al., 2015; Safonova et al., 2016).

The basalts related to OPS sediments have been discovered in several locations within the central Mino terrane on Honshu Island. Safonova et al. (2015) reported findings of basalts associated with OPS sediments in the Nagara River (Early Permian), Neohigashidagawa River (Middle Triassic), and Kiso River. In the Nagara River, outcrops of the OPS Sequence reveal basalts occurring as blocks, accompanied by deep-sea cherts containing microfossils from the Middle Triassic, as documented by (Wakita, 2012). On the other hand, the Neohigashidagawa River exhibits Basaltic rocks within the OPS Sequence that are either covered by Early Permian radiolarian-bearing chert or occur as blocks within Middle Permian carbonates, as reported by Sano (1988a and 1988b). As Safonova et al. (2015) documented, the basaltic bodies discovered in the Kiso River exhibit a thin and elongated shape. These bodies are found interlayered with deep-sea red chert that contains Late Triassic conodonts and radiolarians, as reported by Hori (1992). However, due to the small size of the bodies and the presence of thin contacts, their precise age is not well constrained.

Consequently, whether these basaltic bodies represent lava flows or intrusive sills remains unclear. Another location where Mino-Tamba-Ashio basalts are found is in Wakasa Bay (Nakae, 2000), located in the northern region of Fukui Prefecture and part of the Tamba Belt. Basaltic rocks originating from the Sekumi and Shimonegori complexes commonly form thick flows associated with chert, according to Nakae (2000) and Safonova et al. (2015). The Sekumi Complex includes limestones containing early to middle Permian fusulinids. At the same time, the Shimonegori basalt is part of a basal large-scale slab consisting of limestone with Late Carboniferous to middle Permian fusulinids, as described by Nakae (2000). The basaltic rocks from all these localities exhibit geochemical affinities to dominatly OIB with (N-)MORB in Inuyama, Shuzan Complex and North Tamba (detailed in Appendix Table 1). They are associated with chert, siliceous shale, limy volcaniclastics, and limestone, suggesting their formation on oceanic islands or seamounts (Safonova, Kojima, et al., 2015). These basaltic rocks are covered by turbidite sandstone that alternates with shales in turbidite succession, often forming massive beds. They occur also as blocks in olistostrome sheets (Hattori, 1982). The ages of the turbidites sandstone identified by Hattori (1982) are early to middle Jurassic.

Paleomagnetic studies on the Inuyama cherts òf the Mino-Tamba-Ashio conducted by Hattori (1982), Shibuya and Sasajima (1986), Oda and Suzuki (2000) and Ando et al. (2001) show paleomagnetic inclination between -36.3 and 46.6 (appendix Table 2). Using data from Shibuya and Sasajima (1986), Oda and Suzuki (2000) and Ando et al. (2001), Boscman et al. (2021) show a positive fold test which indicates low-latitude depositional environments (between 15°S and 30°N). Within paleolatitude 20°N, during the time of accretion of the Inuyama cherts (at ~170 Ma), the inner zone subduction system was located at ~52°N (Boschman et al., 2021) – detailed in Appendix Table 2.

Chichibu OPS is distributed over a distance of 1500 km from the Kanto Mountains in the NE through Shikoku and Kyushu to the Ryukyu islands in the SW. From a north-to-south, the Chichibu

accretion complex OPS can be divided into three sub-belts based on their characteristic features and geological structures: the Northern Chichibu (Kashiwagi and Kamiyhosida Units), and Southern Chichibu (Sambosan Unit) (Figure 7). It contains a Jurassic–Early Cretaceous accretionary complex hosting Triassic–Jurassic OPS units and Jurassic accreted mafic–ultramafic igneous complexes of the Mikabu greenstone belt (e.g., Ozawa, Murata, & Itaya, 1997; Ozawa, Murata, Nishimura, et al., 1997). Triassic dominates the OPS sequence of this Chichibu ACs–Jurassic coherent OPS units of chert, siliceous mudstone, and sandstone (the Northern Chichibu of Togano unit) and Jurassic–Early Cretaceous olistostromes with Triassic–Jurassic mafic volcanic rocks, olistostrome, limestone, chert, and limestone bearing clastic sediments (in the Sambosan belt of the Southern Chichibu) (Onoue et al., 2004; Safonova, Kojima, et al., 2015; Endo, 2017; Endo & Wallis, 2017).

Basaltic rocks belonging to the Southern Chichibu OPS have been discovered at the Koguchi site, located in the Sambosan belt near the Kumagawa River in the Yatsushiro district of Kumamoto Prefecture, Kyushu Island, as reported by Safonova et al. (2015). The volcanic rocks at the Koguchi site have a thickness of approximately 40 meters and are primarily composed of basalts and basaltic volcaniclastics. They are associated with Late Triassic limestone and chert. Blocks of volcanic rocks at the site are cemented by a carbonate matrix and are interbedded with lavas and hyaloclastic rocks, according to Onoue et al. (2004). Geochemical analysis conducted by Onoue et al. (2004) and supported by Safonova et al. (2015) indicates that the basaltic rocks from this area exhibit affinities to Oceanic Island Basalts (OIBs).

In the Northern Chichibu, Endo (2017) reported the presence of basaltic rocks within the OPS sequence at the Kunimiyama mine and Kawanokawa mine in Shikoku Prefecture. These rocks are part of the Sumaizuku unit and are primarily composed of altered massive lava associated with stratiform iron-manganese ore deposits. The basalt blocks and layers are often associated with jasper lenses and exhibit pillow basalt and massive textures (Endo, 2017; Endo & Wallis, 2017). Early Permian conodont and radiolarian fossils were identified in red chert near the Kunimiyama deposits and red chert associated with basaltic lavas at various locations in central Shikoku (Fujinaga & Kato, 2005). Geochemical analyses conducted by Nozaki et al. (2005) revealed that the basaltic rocks associated with the Kunimiyama deposits have a normal mid-ocean ridge basalt (N-MORB) origin (Hisada et al., 2016), while some samples also display affinities to enriched MORB and oceanic island basalt (OIB) (Safonova et al., 2016). In addition to OPS in Shikoku Prefecture, the Kamiyoshida Unit and Kashiwagi Unit of the Northern Chichibu have also been discovered in Kanto Mountain (Hisada et al., 2016; Tominaga et al., 2019; Tominaga & Hara, 2021) – *Figure 7*. The basaltic rock of the Kamiyhosida unit is commonly associated with Carboniferous to Permian limestone (Matsuoka et al., 1998; Hisada et al., 2016; Tominaga & Hara, 2021), yet the Kashiwagi Unit also contains Triassic limestone (Igo, 1980; Hisada, 1988). Geochemical affinities of the basaltic rock of these units show OIBs affinities; however, the Kashiwagi Unit also shows OIPB affinities (Tominaga & Hara, 2021). Tominaga et al. (2019 and 2021) suggest the basalt is Carboniferous and Permian seamounts with capping carbonates. Based on

radiolarian fossils in the red shales, the Kamiyoshida Unit's trench-fill sediments were deposited during the late Middle Jurassic (Bajocian to Callovian), implying that the Kamiyoshida Unit was accreted in the late Middle Jurassic or later (Matsuoka et al., 1998; Hisada et al., 2016; Tominaga & Hara, 2021). The Kashiwagi unit is covered by sandstone with depositional age of detrital zircon U–Pb dating between 129 Ma and 125 Ma (Early Cretaceous) (Tominaga et al., 2019). The K–Ar age of the tuffaceous slate is 116.9 ± 2.7 Ma (Hirajima et al., 1992).

Kirschvink et al. (2015) presented paleomagnetic data from Chichibu OPS limestones at Kyushu, showing a paleolatitude at 12.2°S. Within this information, Boschman et al. (2021) reconstructed these limestones at the time of accretion (at ~160 Ma) at paleolatitude from 11°S to 14°S, the outer zone subduction system was located at ~34°N – detailed in Appendix Table 2.

In addition to the Chichibu OPS, the OPS also found in Mikabu Greenstone – has been recently renamed as the Mikabu Unit (Endo & Wallis, 2017) with distribution in Toba Complex, Asama Mountain and Kanto Mountain (Agata, 1994). The ages of the basaltic rocks in Toba Complex identified Kimmeridgian - 154.6 Ma (Sawada et al., 2019) with geochemical affinities N-MORB and OIB (Agata, 1994; Ichiyama et al., 2014; Safonova, Kojima, et al., 2015). Basaltic rock in Asama Mountain reporting the Late Permian age of Gabbro (Agata, 1994) within OIB afinities (Safonova, Kojima, et al., 2015), and Basalt of Mikabu Unit in Kanto Mountain reporting earlies Early Triassic (Hettagian - 199.4 Ma) (Ozawa, Murata, Nishimura, et al., 1997), Middle Triassic (U-Pb, 157 ± 0.9 Ma) (Tominaga & Hara, 2021) with N-MORB affinities (Ozawa, Murata, & Itaya, 1997; Safonova, Kojima, et al., 2015) and OIPB afinities (Tominaga & Hara, 2021). Basaltic rock in the Mikabu Greenstone complex covered by sediment with depositional ages have been inferred from zircon U–Pb dating: 134.2 ± 1.5 Ma (Berriasian–Valanginian; Early Cretaceous) for the tuffaceous slate; 128.2 ± 1.4 and 126.7 ± 2.0 Ma (Barremian; Early Cretaceous) for the sandstone (Tominaga et al., 2019) – *Figure 7*.

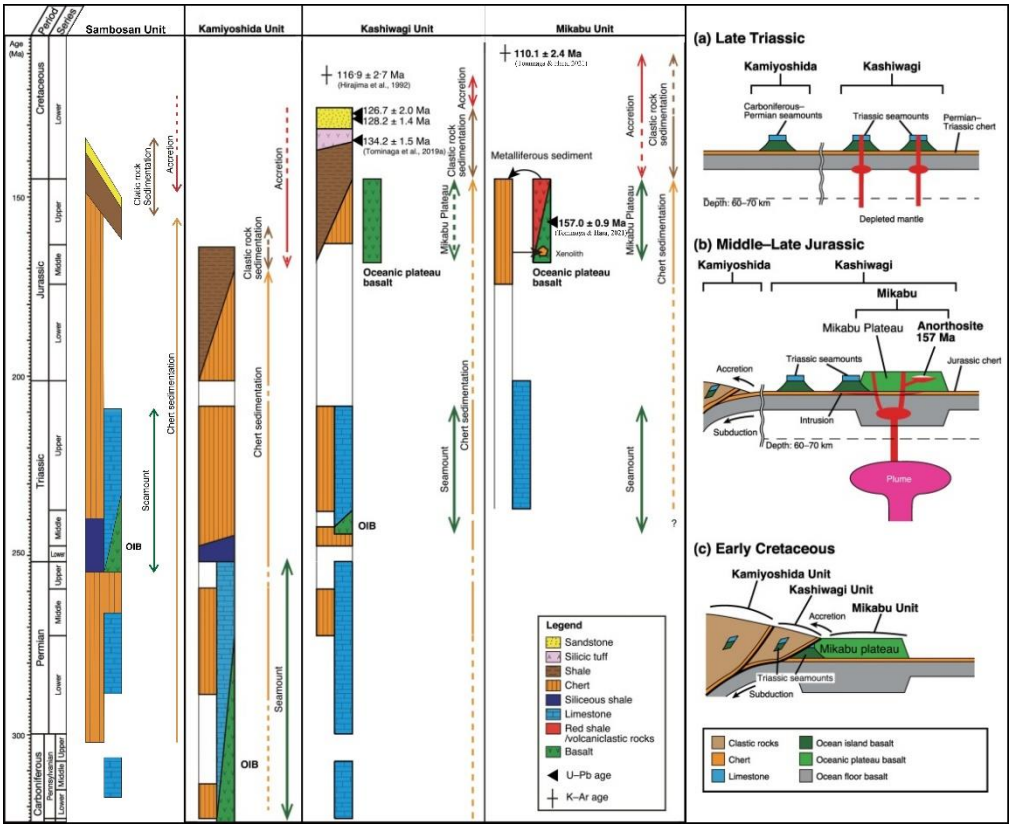

Figure 7. Ocean plate stratigraphy of the Mikabu, Kashiwagi, and Kamiyoshida units and Schematic tectonic evolution of the oceanic plate (After Matsuoka, 1995; Tominaga & Hara, 2021)

Shimanto OPS is one of the best examples of western Pacific accretionary complexes. The age of accreted units ranges from the Late Cretaceous to Neogene (e.g., Kimura & Mukai, 1991; Saito et al., 2014; Taira et al., 1988). The Shimanto belt is categorized into the Cretaceous Northern Shimanto belt and the Paleogene-Neogene Southern Shimanto belt. The Northern Shimanto AC, consisting of OPS sequence range from Early to Late Cretaceous age, comprises two main components: the mélange and flysch units. The mélange consists of blocks of oceanic rocks like pillow basalt, chert, siliceous shales, and similar materials embedded within a sheared argillaceous matrix. In contrast, the flysch comprises terrigenous clastic sediments such as turbiditic sandstone, siliceous shale, and mudstone (Taira et al., 1988; Nakagawa et al., 2009). According to Safonova et al. (2016), north-dipping thrust faults tectonically imbricate the turbidites and the mélanges are highly sheared due to tectonic mixing and occur in a thin tectonic zone between two flysch units.

OPS in the Northern Shimanto accretionary complexes (ACs) at Sumiyoshi Beach in Kochi Prefecture, Shikoku Island, crop out the Pillow Lava (Dolerite and Diabase) with Late Mesozoic age (Safonova et al., 2015) is associated with chert, siliceous, shale. The pillow basalts are intercalated with limestone and are underlain by chocolate chert and shale (Yamamoto, 1987). The ages of the pillow basalt are of Early Cretaceous age (Taira et al., 1988; Nakagawa et al., 2009). Taira et al. (1988) and Isozaki et al. (1990) reported that the basaltic rocks in contact with the Late Cretaceous red chert and mudstone exhibit OIB in geochemical affinities, a finding supported by Safonova et al. (2015).

In **Hokkaido Island,** we found a Late Jurassic accretion complex consisting of exotic blocks of Carboniferous-Triassic limestone and chert (Kawamura, 1986; Ueda, 2003; Ueda & Miyashita, 2005). In the central region of Hokkaido, Cretaceous-Early Paleogene accretionary complexes are frequently overlain by sediments from fore-arc basins. OPS sequence can be found in the Sorachi-Yezo belt in Central Hokkaido and is composed of submarine effusive basalts, pelagic cherts and limestones, and hemipelagic to terrigenous sediments (Kawamura, 1986; Kiminami et al., 1990; Ueda, 2003; Ueda & Miyashita, 2003, 2005). It includes the Kamuikotan metamorphic rocks of pelitic and basic schists yield K-Ar radiometric ages ranging from ~135-50 Ma with a peak at 65 Ma (Sakakibara & Ota, 1994) – which can be used to determine the ages of accretion.

Basaltic rocks belonging to the OPS unit of the Sorachi-Yezo belt are found in the Middle Cretaceous Oku-Niikappu Complex in Central Hokkaido, specifically in the Niikappu River, as reported by Ueda and Miyashita (2002 and 2003). In the Niikappu River, the basaltic rocks of the Oku-Niikappu Complex are observed as tectonic blocks that consist of basal volcanic rocks alternating with conglomerates and cherts (Ueda, 2003). Furthermore, Ueda and Miyashita (2003) discovered sheeted dikes within the tectonic slices of the gabbro-diabase facies, with varying thicknesses ranging from approximately 10 cm to 15 m. The geochemical affinity of the basaltic dikes of the Oku-Niikappu Complex exhibits a Mid-Ocean Ridge Basalt (MORB)-like. In contrast, other igneous rock affinities found are Island Arc (IA/IAT) and Island Arc Basalt (IAB) affinities (Ueda & Miyashita, 2005).

Paleomagnetic studies in these OPS have been done on Oku-Niikappu chert by Boschman et al. (2021) – which show an inclination of 7.2°, corresponding to a paleolatitude of 3.6°N. Following this, Boschman et al. (2021) reconstructed these OPS at the time of accretion (at ~100 Ma) at paleolatitude from 1°N to 5°N, the outer zone subduction system was located at ~54°N – detailed in Appendix Table 2.

- **Philippines**

Accretionary complexes hosting OPS formations in the Philippines in Jurassic accretionary complexes are reported from North Palawan, the Calamian Islands, and South Mindoro Island in the Philippines(Isozaki, 1988a; Faure & Ishidat, 1990; Zamoras & Matsuoka, 2001). They are components of the North Palawan Block (Isozaki, 1988a) and comprise chert, limestone, siliceous mudstone, and turbidite (Zamoras & Matsuoka, 2001). Within the North Palawan Block, the Busuanga Island complex is divided into three distinct belts, the Northern, Middle, and Southern Busuanga Belts, each with its own geological and intricate structural features. The OPS sequence in the Northern Busuanga Belt shows the basaltic sequence in the Bicatan melange complex located in the Bicatan Peninsula. Bicatan melange consists of two sequences: Limestone-basalt-chert or sandstone-chert-mudstone, as Zamoras and Matsuoka (2001) reported. Limestone-basalt-chert melange is poorly layered and composed of highly indurated micritic limestone and basalt with minor bedded chert. Limestone clasts generally have

larger sizes and basalt smaller sizes. Matrix composed of limestone and basalt; the proportion of the coarser limestone-dominated portion occurs in the upper section while the finer basalt-dominated portion occurs at the base of the section; the limited chert component, of probably Permian age, appears immediately above the basalt-dominated portion. The basalt-dominated portion comprises volcaniclastics, occasionally with olivine basalt cobble-sized fragments in a similarly basaltic matrix. Its apparent thickness is approximately 100 m. The ages of chert in North Palawan ACs range form Middle Triassic – Early Cretaceous (Zamoras & Matsuoka, 2001, 2004; Marquez et al., 2006), limestone Middle Permian to Late Jurassic that are scattered around the Calamian group of islands. Trench fill turbidite consists of silicious mudstone and terrigenous mudstone, sandstone, and conglomerate, which shows the Late Jurassic - Early Cretaceous ages (Zamoras & Matsuoka, 2001).

In addition to the Bicatan Melange, the OPS sequence was exposed in Panay Island in the Panicuan Melange. It crops out along the San Jose River west of Iloilo City. Panincuan Melange consists of serpentized peridotites, gabbro, sandstone, and ribbon chert with a greenish silty matrix, as reported by (Yumul, Dimalanta, Gabo-Ratio, et al., 2020). Mafic and Ultramafic block is identified as a part of the Antique Ophiolite within sheeted dikes, basalt sheet flows, and pillows basalt conformably by overlain chert beds; the volcanic sequence of basalts and diabases (gabbro) is mostly olivine tholeiites with transitional (T)-MORB, normal (N)-MORB, and intermediate MORB-IAT geochemical signatures, as reported by Tamayo et al. (2001). Late Cretaceous (Barremian – Aptian) radiolarian fossil has been discovered by Rangin et al. (1991) and Yumul et al. (2020); nanno fossil found discovered in melange matrix show Middle Miocene (Tamayo et al., 2001).

Oceanic floor remnants are also found in the ophiolite and ophiolitic complex. OPS sequence shows in Acoje Block of the Zambales Ophiolite in Zambales range. Acoje block comprises residual harzburgite suite with a thin transition zone dunite; the mafic cumulate sequence comprises troctolite-gabbro. Acoje block is overlain directly in contact with the oldest sedimentary sequence in the northern Zambales, as reported by Queaño et al. (2017) and Yumul et al. (2020). Coarse ophiolite-derived clastic sediments comprise the formation that unconformably overlies the peridotites of the Acoje Block as cropped out in Cabaluan River. Clastic unit mostly shows the interbedded conglomerate and sandstone; conglomerate consists of peridotite with minor gabbro; in some sections, it crops out the coherent sequence of conglomerate overlain with a chaotic sequence composed of red, ribbon bedded chert blocks (olitstolith) with sandy and muddy matrix (Queaño, Dimalanta, et al., 2017). Queaño et al. (2017) discovered the Late Jurassic to Early Cretaceous radiolarian in olitstolith; foraminifera of the sandstone within this sedimentary formation shows the late Early to early Middle Miocene.

In addition to Acoje Block, the OPS sequence is found in Dos Hemanos Island. The OPS was exposed in the Dos Hermanos Melange in Bagui and Ilocos Norte. The component of this melange comprised of peddle- to copebble- clast of peridotite, gabbros, greenschist and mica schist and also radiolarian chert (Late Jurassic – Early Cretaceous); shows highly sheared serpentinite matrix (Queaño,

Marquez, et al., 2017; Pasco et al., 2019; Yumul, Dimalanta, Gabo-Ratio, et al., 2020). Based on the reconstruction OPS from the melange (Wakita & Metcalfe, 2005), we can identify the OPS sequence of the Dos Hemanos Melange consists of the basaltic rock, chert, and turbidite sedimentary (Aksitero Formation).

Basaltic rock of Dos Hermanos Melange identified as MOR (troctolite clast) and IAT (gabbro and gabbro olivine) (Pasco et al., 2019) with ages of these rocks probably older than Late Jurassic (age of radiolarian chert). The Dos Hemanos Melange was identified as a part of the supra-subduction zone (SSZ) Zambales Ophiolite Complex (Pasco et al., 2019) which probably was obducted in older than Late Eocene (U-Pb silicic rock; fossil assemblages of the oldest sedimentary formation – Amato, 1965; Encarnación et al., 1993; Yumul et al., 1998; Yumul, Dimalanta, Salapare, et al., 2020).

- **Costa Rica**

The Santa Rosa Accretionary Complex in the Santa Elena Peninsula hosts an OPS sequence, along with dolerite sills and dikes, as well as massive and pillow basalts; contains Jurassic to Cretaceous radiolarian cherts (Frisch et al., 1992; Donnelly, 1994; Meschede & Frisch, 1994). Santa Rosa Accretionary Complex, which is located beneath the Santa Elena Ultramafic Nappe, is exposed in the Potrero Grande area of the Middle Cretaceous Accretionary Complex in the SW Caribbean plate tectonic window, which is also present in various half-windows along the Santa Elena Peninsula's southern coast (Azéma & Tournon, 1980; Azéma et al., 1982; Tournon & Alvarado, 1997).

The Santa Rosa Accretionary Complex (SRAC) OPS sequence can be obtained along the coastline at Sitio Santa Rosa. Baumgartner and Denyer, (2006), Bandini et al. (2011) and Boschman et al. (2021) reported that pillow basalt, chert and tubidite sequence found in Sitio Santa Rosa, Playa Carrizal and Northern Playa Naranjo. However, Baumgartner and Denyer, (2006) reported the limestone crop out in Northern Playa Naranjo. OPS found at Sitio Santa Rosa are vesicular pillow and massive alkaline basalt, alkaline basaltic sills and dikes cross-cut the Early Jurassic radiolarian chert that overlies a basalt breccia and tuffaceous mudstone, as reported by Baumgartner and Denyer, (2006) and further Boschman et al., (2021), and layered gabbro crop out in the Bahia Nanchite, apart of Santa Elena Nappe, as reported Boschman et al., 2021. Radiometric $^{40}Ar/^{39}Ar$ dating of the basaltic rock shows 124 ± 4 Ma (layered gabbro), and ~175 Ma (basalt sills of the SRAC) (Hauff et al., 2000; Boschman et al., 2021). The geochemical affinity of basalt sills and dikes of SRAC shows the oceanic island basalt (OIB), layered gabbro in Bahia Nanchite shows similar affinities with the pillow basalt from the Santa Elena Ophiolite was mid-ocean ridge basalt (MORB) (Hauff et al., 2000; Gazel et al., 2006). Badini et al. (2011) and Baumgartner & Denyer (2006) documented that the trench-fill sediment of the SRAC is composed of centimeter-bedded volcaniclastic turbidites interspersed with brown siliceous mudstones. This arrangement forms an upward-coarsening sequence, culminating in metric to decametric strata of

debris flows. This sequence spans approximately 150 meters in thickness, extending from the late early Albian to the late early Turonian (Bandini et al., 2011).

- **Mexico**

Mexico OPS is hosted by an accretionary complex in Baja California, Cedros Island, Vizcaino Peninsula, and Margarita Magdalena (Rangin, 1978; Boschman et al., 2021). Cedros Island is predominantly composed of a Late Jurassic melange, resembling the Franciscan melange, which is in close tectonic contact with the ophiolite and the overlying sedimentary sequence ranging from the Middle Jurassic to the Late Cenozoic (Kilmer, 1977; Kimbrough, 1982; Sedlock, 1988; Sedlock & Isozaki, 1990). OPS sequence in this island is found in the Late Jurassic melange (Cedros Formation, Cabo San Augustin and Punta Prieta Ridge) (Kimbrough, 1989). The melange unit on Cedros Island consists of a mixture of different rock types, including graywacke, shale, chert, volcanic rocks, limestone, serpentinite, amphibolite, and glaucophane schist (Kilmer, 1977). Radiolarian chert shows the Late Jurassic – Early Cretaceous (Jones et al., 1976; Kilmer, 1977). Moreover, in Cedros Island, a blueschist-bearing serpentinite-matrix mélange is exposed that contains 1 to 50 m scale blocks of (meta-) basalt, chert, limestone, and upper Lower Cretaceous (105 Ma) turbiditic sedimentary rocks (Rangin, 1978; Sedlock, 1988). The mélange on Cedros Island is a component of a larger collection of Mesozoic rocks associated with subduction processes, including a Triassic SSZ ophiolite, Jurassic arc magmatic rocks, and Cretaceous forearc deposits found across the Vizcaíno-Cedros region in central Baja California (Kimbrough & Moore, 2003).

Hagstrum and Sedlock (1992) conducted a detailed study on the rocks of southeastern Cedros Island, discovering the presence of pillow basalts and chert beds within a continuous section. This section comprised approximately 40 meters of red radiolarian ribbon cherts and 250 meters of thin-bedded turbidites, all belonging to the mélange. By analyzing radiolarian biostratigraphy, they determined that the cherts represented a condensed stratigraphic sequence spanning the Late Triassic to the Early Cretaceous (Sedlock & Isozaki, 1990). Kienast and Rangin (1982) exposed the OPS sequence in a melange unit near Cedros and El Wayle Villages; it shows coherent units, poorly folded, included sheeted dikes, pillow-lavas, bedded cherts, and a volcaniclastic sequence with tuffaceous interbeds and chaotic units of the melange-type arc formed of more or less metamorphosed graywacke, bedded chert basalt and marble blocks engulfed in a poorly metamorphosed or unmetamorphosed sedimentary matrix. The geochemical composition of the pillow basalt in Cedros Island was identified as MORB (Rangin et al., 1983; Kimbrough & Moore, 2003)

The Vizcaino Peninsula has ophiolite complexes that have OPS sequence in subduction melange – which is similar to Cedros Island, in Punta Eugenia (Northen Vizcaino Peninsula), and Puerto Nuevo and Punta San Hipolito (Southern Vizcaino Peninsula) (Kimbrough & Moore, 2003). The OPS sequence well preserved in Southern Vizcaino Peninsula comprises serpentinized harzburgite-dunite

tectonite, gabbro, dykes, sills, and pillow basalts that are overlain by chert, limestone, and tubidite sequence consisting of sandstone and olistostrome (Kimbrough & Moore, 2003; Boschman et al., 2018). Similar sequences also occur in the Northern Vizacaino Peninsula; however, in this region, there is no pelagic sedimentary rock in the OPS sequences (Kimbrough & Moore, 2003). The chert member of the Vizcaino Peninsula dates back to the Late Triassic to Early Jurassic (Rangin et al., 1981). Ages of the basaltic rocks of these OPS are probably older than the Late Triassic; meanwhile, U-Pb of Zircon dating show 221 ± 2 Ma in plagiogranite (Kimbrough & Moore, 2003) and 220 ± 2 Ma dike gabbro (D. A. Barnes & Mattinson, 1981). Sandstone turbidite member of the OPS of the ophiolite melange in Punta Eugenia 141.5 ± 3 Ma (U-Pb on zircon; Hickey, 1984), identified as the ages of the extension of the North American Plate (Boschman et al., 2018). The ages of the accretion of these OPS are probably similar to the ages of accretion on Cedros Island at Albian (at ~105 Ma; Sedlock, 1988).

Paleomagnetic studies of the OPS in Baja California have been done by Boschman et al. (2018 and 2021). The inclination of the Cedros Chert is between -10 ± 13.6° and 5.5 ± 22.3°; at the time of accretion (~105 Ma), Cedros Island was located at 32°N – which was reconstructed in paleolatitude 2.6°S (Boschman et al., 2021). The paleomagnetic Vizcaino Peninsula has been observed in San Hipolito chert and sandstone – the inclination is 43.7 ± 4.5° and 24.0 ± 6.3° respectively, and the pillow lavas show -3.8 ± 8.1° (Boschman et al., 2018) – detailed in Appendix Table 2.

- **California**

Californian Mesozoic OPS is hosted by the Franciscan Subduction Complex, Coast Range Ophiolite, and Great Valley of the Coast Ranges California (Wakabayashi, 2011, 2017; Kusky et al., 2013). The Franciscan subduction complex is structurally overlain by the Coast Range ophiolite consisting of serpentinized ultramafic rocks, mafic to felsic plutonic and volcanic rocks, and chert. Above the ophiolite, there are depositionally overlain forearc basin deposits known as the Great Valley Group, predominantly consisting of well-bedded sandstones and shales, as documented by various studies (e.g., Hamilton, 1969; Ingersoll, 1978; Hopson et al., 1981, 2008; Wakabayashi, 1992). Wakabayashi (2015, 2017) reports that the three mega units, namely the Franciscan subduction complex, the Coast Range ophiolite, and the Great Valley Group, have a combined outcrop length of over 700 km along the strike and 100 km across the strike. The Franciscan Complex was formed through the process of off-scraping and tectonic underplating, involving the accretion of rocks from an east-dipping subduction plate on the eastern Pacific margin, spanning a time period from 160 million years ago to less than 20 million years ago and well-known for its significant occurrence of high-pressure-low-temperature metamorphism (Wakabayashi, 1992, 2011, 2015, 2017; Ernst, 2011).

OPS in the Franciscan complex is well explained by Kusky et al. (2013) and Wakabayashi (2017); it shows (serpentinite) – basalt – chert and/or limestone – clastic or non-clastic sequences—basalt-chert-clastic sequences found in Marin Headlands (Wahrhaftig, 1984). In the Marin Headlands, there is a

sequence of rocks where MORB pillow basalt is overlain by radiolarian chert, which is further overlain by greywacke (Murchey & Jones, 1984; Isozaki & Blake, 1994; Wakabayashi et al., 2010; Ghatak et al., 2012). The melange within OPS sequence crop out in Sunol Regional Wilderness and the Pacheco Pass area of the Northern Diablo Range shows a contact between metagraywacke-metachert and metagraywacke-fine-grained blueschist (metavolcanic), shale matrix within garnet-amphibolite (eclogite) and serpentinite block shows in between, as documented by Wakabayashi (2011). The OPS sequence in the Marin Headlands exhibits a higher proportion of basalt and chert than clastic sedimentary rocks. At the same time, other areas like the Sunol Regional Wilderness or the Pacheco Pass areas of the northern Diablo Range are predominantly dominated by clastic sedimentary rocks (e.g., (Ernst et al., 2009; Wakabayashi, 2017). Pillow basalt in Marin Headlands shows green on dark green on fresh surfaces; red, brown, or yellow where well-defined weathered pillows in some places such as Point Bonita, as Konigsmark (1998) described. The chert found in Marin Headlands is up to 80 m thick (Murchey, 1984; Wahrhaftig, 1984), which explains the ages of the OPS in this region range Pliensbachian (~191 Ma) to Cenomanian time (~94 Ma). The age of greywacke in Marine Headlands is Cenomanian (Murchey, 1984). Nicasio Reservoir terranes is another location that shows the basalt-chert-clastic sequence (Wakabayashi, 2017). However, this region differs from the Marin Headlands sequence. It shows OIB affinity basaltic rocks of pillow basalt and gabbro (Ghatak et al., 2012; Schnur & Gilbert, 2012), and the ages of basaltic rock in this region is ~Berrisian (~140 Ma) (Murchey & Jones, 1984).

Accretionary OPS are found in Permanente Terrane (Sliter, 1984; Larue et al., 1989; Kusky et al., 2013; Wakabayashi, 2017). Sliter (1984), Murchey and Jones (1984), and Larue et al. (1989) documented the occurrence of limestone (up to 130 m thick) within the Permanente Terranes is interbedded with chert, where it overlies OIB basalt (Ghatak et al., 2012) and is overlain by greywacke. However, limestone is less common than chert in the Franciscan complex (Blake Jr et al., 1984; Sliter, 1984). The ages of the limestone in Permanente Terranes range from early Aptian to Turonian (Sliter, 1984; Larue et al., 1989). Basaltic rocks of this OPS sequence are cropped out in the Linda Mar (Pacifica) as a metabasalt block, including chert sandstone graywacke and shale matrix, as Wakabayashi (2011) documented. According to Larue et al. (1989), metabasalt in the Pacifica Quarry predominantly exhibits a massive texture with well-preserved features, while basaltic sills and dikes are locally cut through limestone. Pillow structures are rare except in blocks within the melange, and some instances of amygdaloidal texture can also be observed.

- **Alaska**

Chugach Terrane in Alaska hosts Mesozoic Oceanic Plate Stratigraphy; the OPS sequence is repeated hundreds of times (Kusky & Bradley, 1999). Kusky et al. (1997) classified the Chugach terrane in south-central Alaska into two uni: accreted ocean floor stratigraphy sequences ranging from fairly

coherent Late Cretaceous trench turbidites to extensively disrupted melange. Chugach Terrane melange unit (MgHugh Complex of Kenai Peninsula and Uyak Complex of Kodiak Islands) complexes are a mix of different rocks, including chert, argillite, greenstone, radiolarian chert, gabbroic rocks, and ultramafic rocks (Clark, 1973; Connelly, 1978; Bradley et al., 1992), graywacke (Clark, 1973; Bradley & Kusky, 1990; Bradley et al., 1992). McHugh Complex is cut bedding and cleavage with the Late Cretaceous Turbidites (Valdez Group) in Turnagain Arm, as reported by Bradley and Kusky (1990) and Kusky et al. (1997)

One of the OPS sequences observed in Grewingk Glacier, in the Seldovia Quadrangle of the southern Kenai Peninsula, shows radiolarian chert depositionally overlies pillow basalt (Kusky & Bradley, 1999). The classic OPS sequence of gabbro-basalt-chert-greywacke is repeated three times. In comparison, the shale-greywacke sequence is repeated four times, occurring over a few hundred meters within a highly structurally complex mélange and small-scale repetitions of the OPS stratigraphy down to the microscopic level (Bradley et al., 1992; Kusky & Bradley, 1999; Kusky et al., 2013). Many of the rocks with basaltic compositions appear in the field as a layered fine-grained light green rock, which thin section analysis reveals as a cataclastically microbrecciated basalt (Kusky & Bradley, 1999). Radiolaria found in the cherts of the McHugh Complex across south-central Alaska have been dated to the Ladinian (Middle Triassic) to Albian-Aptian (mid-Cretaceous) periods (S. W. Nelson & Blome, 1991). Within the McHugh Complex, there are scattered blocks of limestone, with the largest ones measuring 50 – 100 m thick and 100 – 200 m long, which are typically buff to light gray in color and have undergone complete recrystallization, as noted by Kusky and Bradley (1999). Some limestone blocks contain Tethyan Permian fusulinids and conodonts of origin, as Bradley et al. (1999) documented, which explained that the basaltic ocean floor ages probably older than or similar to Permian.

Further, the Uyak Complex in Kodiak Islands shows that gabbroic, an ultramafic rock, occurs in the northwesternmost of Kodiak Island as kilometer-sized slabs contain layered gabbro, clinopyroxenite, dunite, and plagioclase peridotite no harzburgite or sheeted dikes, which show fault bounded and serpentinization, as reported by Connelly (1978), Connelly et al., (1977) and Farris (2009 and 2010). Greenstones (metabasite) generally occur as fault-bounded blocks tens to hundreds of meters in size. Non-vesicular pillowed greenstone with a thin chloritic interpillow matrix is the most common, but massive greenstone occurs locally. The greenstones are partially altered to chlorite, albite, pumpellyite, and calcite, but relict phenocrysts of plagioclase and clinopyroxene locally are recognizable (Hill & Gill, 1976; Connelly, 1978). Fossils in the Uyak Complex are rare and range in age from the mid-Permian to the mid-Early Cretaceous (Connelly, 1978).

U-Pb of zircon of Chugach Terrane has been dated by J. M. Amato and Pavlis (2010), depositional ages of the sedimentary cover range from 146 ± 5 Ma and 157 ± 3 Ma (Mesomélange) and

from 84 ± 3 Ma to 91 ± 2 Ma (Graywacke-conglomerate). This age was identified as multiple accretion times in Chugach Terrane in the Late Jurassic – Early Cretaceous and Late Cretaceous, respectively (J. M. Amato & Pavlis, 2010). The ages of the basaltic rock of the Chugach Terrane melange complexes identified Middle Triassic to Early Triassic (McHugh Complex), and the ages of the Basaltic rock in the Uyak Complex identified Middle Permian.

Geochemical analyses of the Uyak Complex indicate the presence of ocean-floor basalt (MORB) according to studies conducted by Hill and Gill (1976) and Nelson and Blome (1991). On the other hand, the McHugh Complex represented a mixture of MORB and enriched MORB (E-MORB), as reported by Nelson and Blome (1991) and (Kusky & Young, 1999).

- **New Zealand**

The Mesozic OPS sequence in New Zealand is identified as hosted by the late Paleozoic-Mesozoic Torlesse terrane. Torlesse terrane of New Zealand is the largest of several subparallel that record more or less continuous convergence at the New Zealand margin of Gondwana from the Permian through to the Mid-Cretaceous consisting predominantly of quartzo-feldspathic sedimentary rocks deposited by sediment gravity flows, basic volcanic rocks which are often associated with colored argillite, chert and limestone, form a minor but conspicuous component, that exhibit complex deformation and low-grade metamorphism (Bradshaw, 1972; Spörli, 1978; MacKinnon, 1983; Bishop et al., 1985).

The Torlesse terrane has been divided into the Rakaia (Permian to late Triassic) and Pahau (latest Jurassic to early Cretaceous) terranes by (Bishop et al., 1985). One OPS sequence was found in exposed rock in the western Aorangi Range in the southernmost part of the North Island of the Pahau terrane. The dominant rock types are interbedded turbiditic greywackes and argillites, with minor conglomerates, metabasite, colored argillite, chert, and melange (George, 1988, 1990). Melange in the Aorangi Range exposed greywacke, chert, and metabasite blocks, which show highly folded (George, 1990). Bradshaw (1973) reported that Torlesse terrane's melange component consists of large limestone (cm-to-m sized), sandstone blocks, pillow lava, red chert, and cherty mudstone. The lava fragments exposed in 30 meters square show the massive and vesicular texture; cherty rocks occur as isolated fragments or as quasi-stratiform strings of lenses with small-scale chevron folding; the matrix of the melange is a dark blue-black mudstone with blebs, streaks, and knots of sandstone (Bradshaw, 1973). Limestone seating on the pillow lava has red tuffaceous bands, also reported by Bradshaw (1973). Late Triassic fossils were found in the limestone blocks, and Late Jurassic fossils were found in the melange matrix (Bradshaw, 1973). Detrital zircon ages 121 ± 3 Ma (Wandres et al., 2005) and 125 ± 5 Ma (Adams et al., 2009) of the Pahau conglomerate matrix in Ethelton indicate a Barremian maximum stratigraphic age for the trench-fill sequence.

Another place exposed to the OPS sequence is on the North Island of New Zealand in Waipapa Terrane. Similar to Terlosse terrane, the Waipapa Terrane comprises tectonically imbricated splitic (pillow) basalts, chert (Permian-Early Jurassic), limestone (Permian), red and green argillite, and trench-fill deposits (Late Jurassic - Early Cretaceous) (Spörli & Grant-Mackie, 1976; Spörli et al., 1989; Kear & Mortimer, 2003; Adams et al., 2007, 2009, 2012; Mortimer et al., 2014).

OPS sequence within this terrane, in the southern part near Auckland, in Weiheike Island and Kawakawa Bay, shows the spilite, chert, and colored argillite overlie younger rocks (terrigenous clastics) (Spörli et al., 1989). Basaltic rocks consist of massive porphyritic lavas, pillow lavas, and breccias and are considered to be tholeiitic metabasalts are associated with chert and shale (Jennings, 1991; Hori et al., 2011). A similar pattern in Whangarei shows spilitic (pillows) basalts and cherts with terrigenous clastic and argillites are mostly Late Jurassic, as well as OPS sequence Tawharanui Peninsula (Aita & Spörli, 1992). The fossils content in the chert section exhibits the Late Triassic and Early Jurassic (Spörli et al., 1989; Aita & Spörli, 1992), further discovery shows Early Triassic fossils in Waiheke Island (Hori et al., 2011). U-Pb of detrital zircon date of graywacke shows 152 ± 1 Ma (Tawharanui), 153 ± 1 Ma (Kawakawa bay) (Adams et al., 2007, 2012)

In addition to OPS in the southern part of Waipapa Terrane, many of the ocean-floor sequences are exposed in the Whangaroa Area in the northern region. OPS in Whangaroa area consists of repetition of spilitic (pillow) basalt, bedded chert, siliceos mudstone, and terrigenous sandstones (greywacke); ocean-floor sequence in the western part of Marble Bay common limestone lenses occasionally appeared on the basalt bodies consist fusulinids (Aita & Spörli, 1992; Takemura et al., 2002; Sakakibara et al., 2003). The ocean floor sequence proportion is smaller in the eastern part of the terrigenous sandstones (Takemura et al., 2002). Radiolarian chert and fusulinids content in limestone explained that the minimum age of pelagic sediment deposition is Late Permian, with the maximum age being Late Triassic. Phosphatic nodules of Late Triassic chert occur in the eastern part of the Mahinepua Peninsula. Basalt in this area is probably Middle Permian in age. Massive and sheeted basalt, discovered in Arrow Island, is overlain red shale and volcanic sandstone; xenolith of red shale found inside the massive basalt; more brecciated basalt, similar to the brecciated basalt in Waiheke Island, shows basalts clast with calcite cement; limestone enclave in hydrofracture basalt with calcite vein, well documented by Sakakibara et al. (2003). This basalt type probably implies that the ages of the basalt intruded into the Middle-Late Permian pelagic sediment is probably Early Triassic. The age of U-Pb from detrital zircon shows 207 ± 4 Ma (near Whangaroa and Marble Bay) (Adams et al., 2007),

The geochemical affinity of spilitic (pillow) basalt rock from the Waipapa Terrane exhibits three different affinities: basalt from Whangarei, Tawharanui Peninsula, Waiheke Island, and Kawakawa Bay exhibits the N-MORB and E-MORB and basalt from Whangaroa Area exhibit the OIB (Jennings, 1991; Black, 1994)

The maximum depositional age of the trench-fill sandstones is constrained through detrital zircon U-Pb ages of 141 ± 2 Ma (near Auckland) to 152 ± 1 Ma (in Northland) (Cawood et al., 1999; Adams et al., 2012).

The Chrystalls Beach Complex consists predominantly of sandstone, interbedded sandstone and mudstone, and lesser amounts of massive mudstone, conglomerate, varicolored argillite, metabasalt, and chert found in southeast Otago, as documented by Nelson (1982) and Hada et al. (2006). The rocks have undergone metamorphism, the grade of which increases progressively northwards from indeterminate prehnite-pumpellyite or pumpellyite-actinolite facies (M. Ito et al., 2000). Metabasalt occurs only within the sheared argillites of the basal parts of the upward coarsening sequences, relatively massive, green metabasalt south of Watsons Beach. (Fagereng & Cooper, 2010) documented two significant blocks of purple metabasalt, each exceeding >100 meters in width: one located south of Akatore Creek and another at Taieri Mouth. The Akatore Fault borders the Taieri Mouth block to the northwest, partially covered by beach sand towards the south. The larger block near Akatore Creek is bounded by faults on both exposed sides. At the same time, smaller but massive metabasalt units are found in various contacts with the surrounding melange, including sedimentary, olistostromal, and tectonic interfaces. The large metabasalt blocks near Akatore Creek and Taieri Mouth exhibit preserved pillow structures, suggesting that these metabasalts originated as pillow lavas. Although often elongated into elliptical shapes due to deformation, the pillows generally retain their overall integrity, while the rims of the pillows commonly display alteration to chlorite-rich mineral assemblages. The Geochemical analyses show that basalt from Taieri Mouth and Watson Beach exhibits MORB affinity, and basalts from Akatore Creek exhibit OIB affinity (Fagereng & Cooper, 2010). Radiolarian chert shows Middle Triassic (Anisian – Ladinian) radiolarians found in phosphatic nodules (M. Ito et al., 2000), indicating the Early-Late Triassic protolith; for progressive graphitization, K-Ar ages of pelitic to semi-pelitic metamorphic rocks that range from 184.6 to 138.7 Ma with 175-155 Ma as peak metamorphism (Nishimura et al., 2000). The ages of trench-fill sediment are speculatively similar to the maximum depositional age of the trench-fill sandstone's detrital zircon U-Pb ages of 221 ± 2 Ma (near Quoin Point) (Adams et al., 2007).

The paleomagnetic study has been conducted by Boschman et al. (2021) on Permian to Early Jurassic radiolarian chert on the Northern Island of New Zealand. The inclination of the Permian and Late Triassci to Early Jurassic ranges from -27.3° to 23.9° and -80.4° to -56.3° (Boschman et al., 2021) and Early Triassic chert -53° (Kodama et al., 2007) – detailed in Appendix Table 2.

Discussion

It is imperative to recognize that volcanic rocks have been preserved within the orogenic belt due to the remnants of oceanic islands formed during the spread of the Panthalassa Ocean. These remnants, most notably attributed to the Izanagi Plate, have been predominantly observed in Japan and Russia,

with potential but minor traces found in the Philippines. The initial ages associated with the inception of the Pacific Ocean Plate and the onset of the Panthalassa breakup are notably discernible in Japanese arcs.

Researchers conducting paleomagnetic studies and paleo reconstructions agree that the early birth of the Pacific plates dates back approximately ~190 Ma. This assertion is supported by Late Carboniferous Oceanic Island Basalt (OIB), suggesting a noteworthy geological activity. This activity was followed by the emergence of a plume, giving rise to another Permian seamount, documented in the Mino-Tamba-Ashio ACs, which reached the continental margin in the Early Cretaceous.

Upon closer examination of our database, we unearthed evidence of Triassic to Late Jurassic MORB-type basalt in Mino-Tamba-Ashio Acs, which could indicate the Panthalassa plate's early fragmentation into the nascent Pacific between 250 Ma and 154 Ma. Most Mesozoic OIB and MORB-type basalt in the Japanese Arc eventually reached the continental margin (Eurasian plates) around the Berriasian to Albian. Within these age determinations, we can reasonably estimate that the Izanagi Plate endured for approximately ~190 million years before manifesting in the Japanese Arc.

In Sakhalin Island, Russian OPS divulged the presence of the Norian age of volcanic rocks and reaching the continental margin in the Early Eocene, which suggests that the subduction history of the Izanagi Plates, as recorded in this region, endured for a notably longer duration compared to the Japanese arcs. The remnants of the Izanagi Plates are also documented in the Philippines within a small fraction of the melange complexes. Identifying Mesozoic volcanic features, particularly basaltic rocks within the OPS sequence in this region, poses a high challenge, similar to the situation in Southeast Asia. Nevertheless, we have identified at least one instance of Mid-Late Triassic OIB within the Bicatan Melange on Calamian Island. This intrusion occurred within Permian-Middle Triassic limestone, and notably, this volcanic rock shares striking similarities with the Togano Group in the Southern Chichibu ACs, a proposition outlined by Zamoras and Matsuoka (2001).

Moving forward to the Farallon Plates, the OPS sequence includes volcanic rocks identified in Mexico on Cedros Island (Melange Complex) and Vizcaino Peninsula (Ophiolite Complex), as well as in Puerto Nuevo Melange and Arteaga Complex. Late Triassic MORB and OIB-type basalt are reported in this region. Both types of volcanic features identified reached the Albian continental (Northern American Plate) margin, which indicates the Farallon plate's longevity in this region was approximately ~115 million years. In our database, in the SRAC, the Farallon plate's identified lifespan was slightly shorter than in Cedros Island, about ~75 million years. This condition, however, was probably longer than ~75 million years unless specific ages of the massive and vesicular pillow basalts below the radiolarian and alkaline basaltic sills are available. Assuming that the massive and vesicular pillow basalts are older than 190 Ma, we can estimate the Farallon plate's long life in SRAC. In the Franciscan complex in California, the Pliensbachian MORB-type of basalt is followed by the Early Cretaceous

OIB and EMORB basaltic rocks. Our findings show that Early Jurassic and Early Cretaceous basaltic rocks in this complex reached the continental margin almost simultaneously during the Cenomanian-Turonian. The time travel of this MORB from the rifting margin varied from 130 million years to 46 million years. The remnants of the Farallon plates also fossilized in Alaska exhibit Middle Permian-Early Jurassic E-MORB type of basalt. This basalt is expected to reach the Northern American Plate margin after varying durations, ranging from 100 million to 155 million years. Utilizing the MORB-type basaltic rock from accreted OPS of Costa Rica, Mexico, California, and Alaska, we can assume that the Pacific probably originated between the Middle Permian and the Middle Jurassic.

The remnants of the Phoenix Plates are well-documented in New Zealand. Most of the MORB-type basaltic rock in this region dates back to the Early Triassic, succeeded by Late Triassic Seamounts. These basaltic rocks from the Late Triassic to Early Cretaceous reached the continental margin. However, one site exhibits the Middle Permian OIB, yet it indicates a brief travel time to reach the continental margin in the Late Triassic. This data suggests that the Phoenix plate was likely completely replaced by the Pacific plate in the early Cretaceous. However, the oldest MORB-type in this region dates back to the Early Triassic, indicating that the Pacific Plate might have emerged between the Early and Late Triassic. This data aligns with the evidence of a Permian seamount in this region, likely arising from the Late Carboniferous subduction and subsequent plume activity as a paleo hotspot.

Based on our findings in the database, we assume that the early birth of the Pacific Plates occurred between the Early to Late Triassic, approximately between 250 and 200 Ma. This timeframe, however, suggests that the age estimates presented in this report are slightly older compared to previous research, which offered a range of 200 to 190 Ma (as indicated by Seton et al., 2012; Müller et al., 2016; Boschman & van Hinsbergen, 2016; Young et al., 2019; Boschman et al., 2021). This distinction can be reconciled with earlier research, provided we consider that the early Pacific Plate's geochemical signature was that of E-MORB, predominantly reflected in our database as Late Triassic to Early Jurassic.

Hotspot distribution in the Paleozoic-Mesozoic

In mantle plumes, diverse definitions abound, with two predominant interpretations. W. J. Morgan originally defined a mantle plume as a slender, heated column of mantle material ascending from the core-mantle boundary. These plumes, also termed mantle source "hotspots," originate from the lower mantle, resulting in the thinning of the overlying lithosphere (Morgan, 1971). Our database indicates a likelihood of the paleozoic-mesozoic MORB and OIB volcanic features being associated with mantle plumes. However, discerning the global distribution pattern of these hotspots during the paleozoic-mesozoic proves challenging in our database without paleogeographic reconstruction. Consequently, by amalgamating our database with paleo reconstructions from Boschman et al. (2021),

Müller et al. (2016), and Seton et al. (2012), we endeavor to ascertain the initial positions of volcanic seamounts between paleozoic and Mesozoic.

Related to the geochemical composition of the seamounts, it is clear that the composition of the paleo seamount has two affinities: MORB and OIB. The MORB was created during the breakdown of the tectonic plate (Panthalassa Plate), followed by the OIB created related to the plume activities, and the E-MORB formed relatively near the original MORB (Figure 8). According to this finding, we can argue that the hotspot beneath the mantle at the Mesozoic is similar to the present hotspot condition.

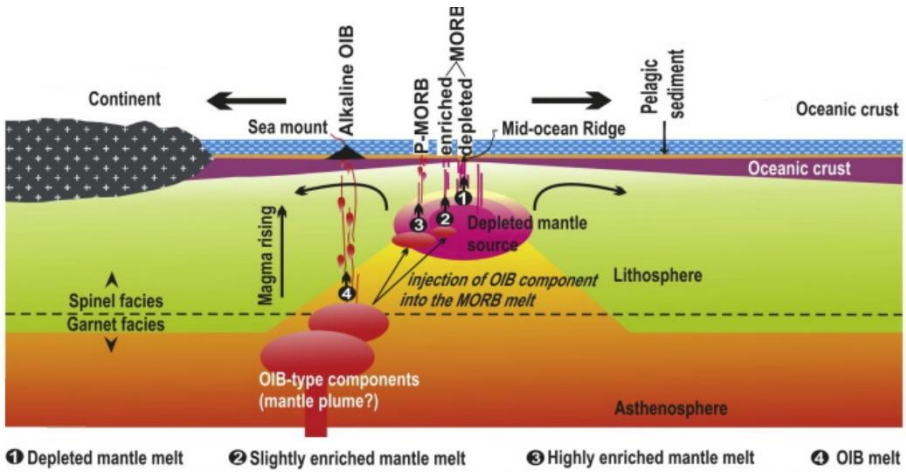

Figure 8. Schematic diagram of the tectonic setting based on geochemical affinities Modified from Khogenkumar et al. (2016)

However, our findings reveal at least 28 volcanic features (11 Late Paleozoic and 17 Mesozoic) within the accreted OPS associated with OIBs or Seamounts in the ancient Pacific Plate. Late Paleozoic to Triassic seamounts in the Japanese Arc exhibit resemblances to the Hawaiian type of OIBs (Safonova, Litasov, et al., 2015; Safonova et al., 2016). However, these seamounts are likely linked with at oceanic hotspot associated with Pacific LLVP near the triple junction of the ancient Panthalassa plate and other EM oceanic hotspots surrounding the Pacific Ocean. On the other hand, Jurassic to Cretaceous seamounts are predominantly identified in different Izanagi and Farallon Plates. Yet, examining paleogeographic maps, it appears that Jurassic OIBs share a similar source with the Triassic Seamounts. In contrast, Cretaceous OIBs seem to originate from distinct ancient hotspots.

Based on our explanation and data, it is plausible that we have identified a slight predominance of Mesozoic hotspot distribution in the southern hemisphere during the Paleozoic to Mesozoic, which aligns with the current Pacific condition, where six EM oceanic hotspots are primarily situated in the southern hemisphere (Morgan, 1971; Li, 2018; Jackson & Macdonald, 2022). The number of oceanic hotspots presumed to exist during the Mesozoic is likely fewer than in the present era. This conclusion reflects the small number of the Mesozoic oceanic seamounts that are preserved in the accreted OPS.

Conclusion

Our extensive analysis of volcanic rocks within the orogenic belt has unveiled a compelling narrative of ancient oceanic remnants linked to the Izanagi Plate. Predominantly concentrated in Japan and Russia. The Izanagi Plate's endurance for approximately ~190 million years before it accreted into the Japanese Arc. Farallon Plates volcanic rocks were identified in various locations, indicating a lifespan of approximately ~115 million years in Mexico and slightly shorter in SRAC. The Phoenix Plates' remnants in New Zealand suggest their likely replacement by the Pacific Plate in the early Cretaceous. The oldest MORB-type in this region dates back to the Early Triassic, implying the Pacific Plate's emergence between the Early and Late Triassic.

Our findings on the early birth of the Pacific Plates based on the geochemical affinity and the ages of the OPS Sequence's volcanic feature and trench fill sediment show different timeframes within previous research. Additionally, we identified a slight predominance of Mesozoic hotspot distribution in the southern hemisphere during the Paleozoic to Mesozoic, aligning with the current Pacific condition.

Indeed, for further research, conducting a more detailed compilation of volcanic features within the accreted OPS is imperative. This comprehensive compilation will provide a robust dataset for in-depth analysis. Additionally, performing dating ages, paleomagnetic, and geochemical analyses on selected volcanic features will significantly enhance our understanding of the distribution of Mesozoic hotspots and shed light on the early formation of ancient Pacific plate boundaries. These analyses will offer valuable insights into the geological processes and tectonic events that shaped the region, providing a more accurate portrayal of its dynamic history. Such research endeavors will undoubtedly advance our knowledge of plate tectonics and the evolution of the Pacific Plate.

Acknowledgments

I would like to acknowledge and warmest to my supervisors, ***Prof. Dr. Douwe van Hinsbergen*** and ***Dr. Lydian Boschman,*** who made this work possible, especially to Prof Douwe. His guidance and advice carried me through all the stages of writing my thesis. I would also like to thank ***Dr. Eldert Lieven Advokaat***, who gave feedback on my thesis. I would also like to thank the ***Educational Fund Management Institution*** **(LPDP)** team for supporting me during my studies at Utrecht University. My family for their continuous support and understanding when undertaking my research and writing my project. Finally, I thank Grammarly and Quillbot for helping me polish my English by giving word choices and suggestions and rephrasing the sentences to improve my writing style.

References

Adams, C. J., Campbell, H. J., & Griffin, W. L. (2007). Provenance comparisons of Permian to Jurassic tectonostratigraphic terranes in New Zealand: perspectives from detrital zircon age patterns. *Geological Magazine*, *144*(4), 701–729. https://doi.org/10.1017/S0016756807003469

Adams, C. J., Mortimer, N., Campbell, H. J., & Griffin, W. L. (2009). Age and isotopic characterisation of metasedimentary rocks from the Torlesse Supergroup and Waipapa Group in the central North Island, New Zealand. *New Zealand Journal of Geology and Geophysics*, *52*(2), 149–170. https://doi.org/10.1080/00288300909509883

Adams, C. J., Mortimer, N., Campbell, H. J., & Griffin, W. L. (2012). Detrital zircon geochronology and sandstone provenance of basement Waipapa Terrane (Triassic–Cretaceous) and Cretaceous cover rocks (Northland Allochthon and Houhora Complex) in northern North Island, New Zealand. *Geological Magazine*, *150*(1), 89–109. https://doi.org/10.1017/S0016756812000258

Agata, T. (1994). The Asama igneous complex, central Japan: An ultramafic-mafic layered intrusion in the Mikabu greenstone belt, Sambagawa metamorphic terrain. *Lithos*, *33*(4), 241–263. https://doi.org/10.1016/0024-4937(94)90032-9

Aita, Y., & Spörli, K. B. (1992). Tectonic and paleobiogeographic significance of radiolarian microfaunas in the Permian to Mesozoic basement rocks of the North Island, New Zealand. *Palaeogeography, Palaeoclimatology, Palaeoecology*, *96*(1–2), 103–125.

Amato, F. L. (1965). Stratigraphic paleontology in the Philippines. *Philippine Geologist*, *20*, 121–140.

Amato, J. M., & Pavlis, T. L. (2010). Detrital zircon ages from the Chugach terrane, southern Alaska, reveal multiple episodes of accretion and erosion in a subduction complex. *Geology*, *38*(5), 459–462. https://doi.org/10.1130/G30719.1

Ando, A., Kodama, K., & Kojima, S. (2001). Low-latitude and Southern Hemisphere origin of Anisian (Triassic) bedded chert in the Inuyama area, Mino terrane, central Japan. *Journal of Geophysical Research: Solid Earth*, *106*(B2), 1973–1986. https://doi.org/10.1029/2000JB900305

Azéma, J., Origlia, I., Tournon, J., & DeWever, P. (1982). Nouvelles données sur la présence de Crétacé Moyen au sein des formations volcano-sedimentaires de l'autochtone relatif de la péninsule de Santa Elena (Costa Rica, Amérique Centrale). *9a Réunion Annuelle Des Sciences de La Terre*, 22.

Azéma, J., & Tournon, J. (1980). La péninsule de Santa Elena, Costa Rica: un massif ultrabasique charrié en marge pacifique de l'Amérique Centrale, Costa Rica. *Comptes Rendus de L'Académie Des Sciences Des Paris*, *290*, 9–12.

Bandini, A. N., Baumgartner, P. O., Flores, K., Dumitrica, P., & Jackett, S.-J. (2011). Early Jurassic to early Late Cretaceous radiolari-ans from the Santa Rosa accretionary complex (northwestern Costa Rica). *Ofioliti*, *36*(1), 1–35. https://doi.org/10.4454/OFIOLITI.V36I1.392

Barnes, D. A., & Mattinson, J. M. (1981). Late Triassic–Early Cretaceous age of eugeosynclinal terranes, western Vizcaíno Peninsula, Baja California Sur, Mexico. *Geological Society America Abstracts with Programs*.

Barnes, P. M., & Korsch, R. J. (1991). Melange and related structures in Torlesse accretionary wedge, Wairarapa, New Zealand. *New Zealand Journal of Geology and Geophysics*, *34*(4), 517–532. https://doi.org/10.1080/00288306.1991.9514487

Baumgartner, P. O., & Denyer, P. (2006). Evidence for middle Cretaceous accretion at Santa Elena Peninsula (Santa Rosa Accretionary Complex), Costa Rica. *Geologica Acta*, *4*, 179–191.

Bazhenov, M. L., Zharov, A. E., Levashova, N. M., Kodama, K., Bragin, N. Y., Fedorov, P. I., Bragina, L. G., & Lyapunov, S. M. (2001). Paleomagnetism of a Late Cretaceous island arc complex from South Sakhalin, East Asia: Convergent boundaries far away from the Asian continental margin? *Journal of Geophysical Research: Solid Earth*, *106*(B9), 19193–19205. https://doi.org/10.1029/2000JB900458

Bishop, D. G., Bradshaw, J. D., & Landis, C. A. (1985). *Provisional terrane map of South Island, New Zealand*.

Black, P. M. (1994). The" Waipapa Terrane", North Island, New Zealand: Subdivision and correlation. *Geoscience Reports of Shizuoka University*, *20*, 55–62.

Blake Jr, M. C., Engebretson, D. C., & Jayko, A. S. (1985). *Tectonostratigraphic terranes in southwest Oregon*.

Blake Jr, M. C., Howell, D. G., & Jayko, A. S. (1984). Tectonostratigraphic terranes of the San Francisco Bay Region. In M. C. J. Blake (Ed.), *Franciscan Geology of Northern California* (Vol. 43, pp. 5–22). Pacific Section, Society of Economic Paleontologists and Mineralogists.

Boschman, L. M., Hinsbergen, D. J. J. van, Langereis, C. G., Flores, K. E., Kamp, P. J. J., Kimbrough, D. L., Ueda, H., Lagemaat, S. H. A. van de, Wiel, E. van der, & Spakman, W. (2021). Reconstructing lost plates of the Panthalassa Ocean through paleomagnetic data from circum-Pacific accretionary orogens. *American Journal of Science*, *321*(6), 907–954. https://doi.org/10.2475/06.2021.08

Boschman, L. M., van der Wiel, E., Flores, K. E., Langereis, C. G., & van Hinsbergen, D. J. J. (2019). The Caribbean and Farallon Plates Connected: Constraints From Stratigraphy and Paleomagnetism of the Nicoya Peninsula, Costa Rica. *Journal of Geophysical Research: Solid Earth*, *124*(7), 6243–6266. https://doi.org/10.1029/2018JB016369

Boschman, L. M., & van Hinsbergen, D. J. J. (2016). On the enigmatic birth of the Pacific Plate within the Panthalassa Ocean. *Science Advances*, *2*(7). https://doi.org/10.1126/sciadv.1600022

Boschman, L. M., van Hinsbergen, D. J. J., Kimbrough, D. L., Langereis, C. G., & Spakman, W. (2018). The Dynamic History of 220 Million Years of Subduction Below Mexico: A Correlation Between Slab Geometry and Overriding Plate Deformation Based on Geology, Paleomagnetism, and Seismic Tomography. *Geochemistry, Geophysics, Geosystems*, *19*(12), 4649–4672. https://doi.org/10.1029/2018GC007739

Bradley, D. C., & Kusky, T. M. (1990). Kinematics of late faults along Turnagain Arm. *Mesozoic Accretionary Complex, South-Central Alaska: US Geological Survey Bulletin*, *1946*, 3–10.

Bradley, D. C., Kusky, T. M., & Ford, A. (1992). Deformation history of the McHugh Complex, Seldovia quadrangle, south-central Alaska. *US Geological Survey Bulletin*, *1999*, 17–32.

Bradshaw, J. D. (1972). Stratigraphy and structure of the Torlesse Supergroup (Triassic-Jurassic) in the foothills of the Southern Alps near Hawarden (S60–61), Canterbury. *New Zealand Journal of Geology and Geophysics*, *15*(1), 71–87.

Bradshaw, J. D. (1973). Allochthonous mesozoic fossil localities in melange within the Torlesse rocks of North Canterbury. *Journal of the Royal Society of New Zealand*, *3*(2), 161–167. https://doi.org/10.1080/03036758.1973.10430598

Cawood, P. A., & Buchan, C. (2007). Linking accretionary orogenesis with supercontinent assembly. *Earth-Science Reviews*, *82*(3), 217–256. https://doi.org/https://doi.org/10.1016/j.earscirev.2007.03.003

Cawood, P. A., Nemchin, A. A., Leverenz, A., Saeed, A., & Balance, P. F. (1999). U/Pb dating of detrital zircons: Implications for the provenance record of Gondwana margin terranes. *Geological Society of America Bulletin*, *111*(8), 1107–1119. https://doi.org/10.1130/0016-7606(1999)111<1107:UPDODZ>2.3.CO;2

Centeno-García, E., Guerrero-Suastegui, M., & Talavera-Mendoza, O. (2008). The Guerrero Composite Terrane of western Mexico: Collision and subsequent rifting in a supra-subduction zone. In *Special Paper 436: Formation and Applications of the Sedimentary Record in Arc Collision Zones* (pp. 279–308). Geological Society of America. https://doi.org/10.1130/2008.2436(13)

Centeno-García, E., Ruíz, J., Coney, P. J., Patchett, P. J., & Ortega-Gutiérrez, F. (1993). Guerrero terrane of Mexico: Its role in the Southern, Cordillera from new geochemical data. *Geology*, *21*(5), 419. https://doi.org/10.1130/0091-7613(1993)021<0419:GTOMIR>2.3.CO;2

Clark, S. H. B. (1973). The McHugh complex of south-central Alaska. *U.S. Geological Survey Bulletin*, *1372–D*.

Condie, K. C., Kröner, A., & Stern, R. J. (2006). Penrose conference report: When did plate tectonics begin? *Geological Society of America Today*, *16*(10), 40–41. https://doi.org/10.1130/1052-5173(2006)16[40:PCRWDP]2.0.CO;2

Connelly, W. (1978). Uyak Complex, Kodiak Islands, Alaska: A Cretaceous subduction complex. *Geological Society of America Bulletin*, *89*(5), 755. https://doi.org/10.1130/0016-7606(1978)89<755:UCKIAA>2.0.CO;2

Connelly, W., Hill, M., Hill, B. B., & Moore, J. C. (1977). The Uyak Complex, Kodiak Islands, Alaska: A subduction complex of Early Mesozoic age. In Manik Talwani & Walter C. Pitman III (Eds.), *Island Arcs, Deep Sea Trenches and Back-Arc Basins* (Vol. 1, pp. 465–466). American Geophysical Union. https://doi.org/10.1029/ME001p0465

Curry, F. B., Cox, A., & Engebretson, D. C. (1984). *Paleomagnetism of Franciscan rocks in the Marin Headlands*.

Dobretsov, M. L., & Kuroda, I. (1969). Geological regularities of glaucophane metamorphism in the northwestern part of the Pacific folded margin. *Geologiya Geofizika*, *12*, 19–41.

Donnelly, T. W. (1994). The Caribbean Cretaceous basalt association: a vast igneous province that includes the Nicoya Complex of Costa Rica. *Profil*, *7*, 17–45.

Encarnación, J. P., Mukasa, S. B., & Obille, E. C. (1993). Zircon U-Pb geochronology of the Zambales and Angat Ophiolites, Luzon, Philippines: Evidence for an Eocene arc-back arc pair. *Journal of Geophysical Research: Solid Earth*, *98*(B11), 19991–20004. https://doi.org/10.1029/93JB02167

Endo, S. (2017). Ilvaite–manganilvaite series minerals in jasper and iron–manganese ore from the Northern Chichibu belt, central Shikoku, Japan. *Journal of Mineralogical and Petrological Sciences*, *112*(4), 166–174. https://doi.org/10.2465/jmps.170408

Endo, S., & Wallis, Simon. R. (2017). Structural architecture and low-grade metamorphism of the Mikabu-Northern Chichibu accretionary wedge, SW Japan. *Journal of Metamorphic Geology*, *35*(6), 695–716. https://doi.org/10.1111/JMG.12251

Ernst, W. G. (2011). Accretion of the Franciscan Complex attending Jurassic-Cretaceous geotectonic development of northern and central California. *Geological Society of America Bulletin*, *123*(9–10), 1667–1678. https://doi.org/10.1130/B30398.1

Ernst, W. G., Martens, U., & Valencia, V. (2009). U-Pb ages of detrital zircons in Pacheco Pass metagraywackes: Sierran-Klamath source of mid-Cretaceous and Late Cretaceous Franciscan deposition and underplating. *Tectonics*, *28*(6). https://doi.org/10.1029/2008TC002352

Escalona, A., Norton, I. O., Lawver, L. A., & Gahagan, L. (2021). Quantitative Plate Tectonic Reconstructions of the Caribbean Region from Jurassic to Present. In *Memoir 123: South America—Caribbean—Central Atlantic Plate Boundary: Tectonic Evolution, Basin Architecture, and Petroleum Systems* (pp. 239–263). AAPG. https://doi.org/10.1306/13692247M1233849

Fagereng, Å., & Cooper, A. F. (2010). Petrology of metabasalts from the Chrystalls Beach accretionary mélange - implications for tectonic setting and terrane origin. *New Zealand Journal of Geology and Geophysics*, *53*(1), 57–70. https://doi.org/10.1080/00288301003631806

Farris, D. W. (2009). Construction and evolution of the Kodiak Talkeetna arc crustal section, southern Alaska. In Miller; Robert B. & A. W. Snoke (Eds.), *Crustal Cross Sections from the Western North American Cordillera and Elsewhere: Implications for Tectonic and Petrologic Processes* (GSA Special Paper, Vol. 456, pp. 69–96). Geological Society of America. https://doi.org/10.1130/2009.2456(03)

Farris, D. W. (2010). Tectonic and petrologic evolution of the Kodiak batholith and the trenchward belt, Kodiak Island, AK: Contact fault juxtaposition? *Journal of Geophysical Research*, *115*(B7), B07208. https://doi.org/10.1029/2009JB006434

Faure, M., & Ishidat, K. (1990). The Mid-Upper Jurassic olistostrome of the west Philippines: a distinctive key-marker for the North Palawan block. *Journal of Southeast Asian Earth Sciences*, *4*(1), 61–67.

Frisch, W., Meschede, M., & Sick, M. (1992). Origin of the Central American ophiolites: Evidence from paleomagnetic results. *Geological Society of America Bulletin*, *104*(10), 1301–1314. https://doi.org/10.1130/0016-7606(1992)104<1301:OOTCAO>2.3.CO;2

Fujinaga, K., & Kato, Y. (2005). Radiolarian Age of Red Chert from the Kunimiyama Ferromanganese Deposit in the Northern Chichibu Belt, Central Shikoku, Japan. *Resource Geology*, *55*(4), 353–356. https://doi.org/10.1111/J.1751-3928.2005.TB00256.X

Gazel, E., Denyer, P., & Baumgartner, P. (2006). Magmatic and geotectonic significance of Santa Elena Peninsula, Costa Rica. *Geologica Acta*, *4*, 193–202. https://doi.org/10.1344/105.000000365

George, A. D. (1988). *Accretionary Prism Rocks of the Torlesse Terrane: Western Aorangi Range–Cape Palliser, New Zealand* [PhD Thesis]. Victoria University of Wellington, New Zealand .

George, A. D. (1990). Deformation processes in an accretionary prism: a study from the Torlesse terrane of New Zealand. *Journal of Structural Geology*, *12*(5–6), 747–759. https://doi.org/10.1016/0191-8141(90)90086-E

George, A. D. (1993). Radiolarians in offscraped seamount fragments, Aorangi Range, New Zealand. *New Zealand Journal of Geology and Geophysics*, *36*(2), 185–199. https://doi.org/10.1080/00288306.1993.9514567

Ghatak, A., Basu, A. R., & Wakabayashi, J. (2012). Elemental mobility in subduction metamorphism: insight from metamorphic rocks of the Franciscan Complex and the Feather River ultramafic belt, California. *International Geology Review*, *54*(6), 654–685. https://doi.org/10.1080/00206814.2011.567087

Gromme, C. S., & Gluskoter, H. J. (1965). Remanent magnetization of spilite and diabase in the Franciscan formation, western Marin County, California. *The Journal of Geology*, *73*(1), 74–94.

Hada, S., Yoshikura, S., Landis, C. A., & Coombs, D. S. (2006). Mélange fabric of the Chrystalls Beach Complex, southeast Otago, New Zealand. *The Journal of the Geological Society of Japan*, *112*(6), 112.6.XI_XII. https://doi.org/10.5575/geosoc.112.6.XI_XII

Hagstrum, J. T., & Sedlock, R. L. (1992). Paleomagnetism of mesozoic red chert from Cedros Island and the San Benito Islands, Baja California, Mexico revisited. *Geophysical Research Letters*, *19*(3), 329–332. https://doi.org/10.1029/91GL02692

Hallam, A. (1986). Evidence of displaced terranes from Permian to Jurassic faunas around the Pacific margins. *Journal of the Geological Society*, *143*(1), 209–216. https://doi.org/10.1144/gsjgs.143.1.0209

Hamilton, W. (1969). Mesozoic California and the underflow of Pacific mantle. *Geological Society of America Bulletin*, *80*(12), 2409–2430.

Harbert, W. P., McLaughlin, R. J., & Sliter, W. V. (1984). *Paleomagnetic and tectonic interpretation of the Parkhurst Ridge limestone, Coastal Belt Franciscan, northern California*.

Hattori, I. (1982). The mesozoic evolution of the mino terrane, central Japan: A geologic and paleomagnetic synthesis. *Tectonophysics*, *85*(3–4), 313–340. https://doi.org/10.1016/0040-1951(82)90108-1

Hauff, F., Hoernle, K., van den Bogaard, P., Alvarado, G., & Garbe-Schönberg, D. (2000). Age and geochemistry of basaltic complexes in western Costa Rica: Contributions to the geotectonic

evolution of Central America. *Geochemistry, Geophysics, Geosystems*, *1*(5). https://doi.org/10.1029/1999GC000020

Hawkesworth, C. J., Dhuime, B., Pietranik, A. B., Cawood, P. A., Kemp, A. I. S., & Storey, C. D. (2010). The generation and evolution of the continental crust. *Journal of the Geological Society*, *167*(2), 229–248. https://doi.org/10.1144/0016-76492009-072

Hayami, I. (1961). On the Jurassic pelecypod faunas in Japan: University of Tokyo. *Journal of the Faculty of Science University of Tokyo*, *13*(2), 243–343.

Hayami, L. (1984). Jurassic marine bivalve faunas and biogeography in Southeast Asia. *Geology and Palaeontology of Southeast Asia*, 229–237.

Hickey, J. J. (1984). *Stratigraphy and Composition of a Jura-Cretaceous Volcanic Arc Apron, Punta Eugenia, Baja California Sur, Mexico*.

Hill, M., & Gill, J. (1976). Mesozoic greenstones of diverse ages from the Kodiak Islands, Alaska. *EOS Transactions American Geophysical Union*, *57*(12), 1021. https://eurekamag.com/research/019/400/019400840.php

Hirajima, T., Isono, T., & Itaya, T. (1992). K-Ar age and chemistry of white mica in the Sanbagawa metamorphic rocks in the Kanto Mountains, central Japan. *The Journal of the Geological Society of Japan*, *98*(5), 445–455. https://doi.org/10.5575/geosoc.98.445

Hisada, K. (1988). Nappe of the Chichibu complex in the Kuroyama area, eastern part of the Kanto mountains, central Japan. *Annual Report of the Institute of Geoscience, the University of Tsukuba*, *15*, 49–53.

Hisada, K., Tominaga, K., Sekine, K., Matsuoka, K., & Kato, K. (2016). Geology of the northern Chichibu belt in the Kanto Mountains, central Japan. *The Journal of the Geological Society of Japan*, *122*(7), 2016.0026. https://doi.org/10.5575/geosoc.2016.0026

Hopson, C. A., Mattinson, J. M., & Pessagno, E. A. J. (1981). Coast range ophiolite, western California. In W. G. Ernst (Ed.), *Geotectonic Development of California* (W.G. Ernst (Ed.), pp. 418–510). Prentice-Hall.

Hopson, C. A., Mattinson, J. M., Pessagno, E. A., & Luyendyk, B. P. (2008). California Coast Range ophiolite: Composite Middle and Late Jurassic oceanic lithosphere. In *Special Paper 438: Ophiolites, Arcs, and Batholiths: A Tribute to Cliff Hopson* (pp. 1–101). Geological Society of America. https://doi.org/10.1130/2008.2438(01)

Hori, R. (1992). Radiolarian Biostratigraphy at the Triassic/Jurassic. *Journal of Geosciences Osaka City University*, *35*, 53–65.

Hori, R., Yamakita, S., Ikehara, M., Kodama, K., Aita, Y., Sakai, T., Takemura, A., Kamata, Y., Suzuki, N., Takahashi, S., Spörli, K. B., & Grant-Mackie, J. A. (2011). Early Triassic (Induan) Radiolaria and carbon-isotope ratios of a deep-sea sequence from Waiheke Island, North Island, New Zealand. *Palaeoworld*, *20*(2–3), 166–178. https://doi.org/10.1016/j.palwor.2011.02.001

Horton, B. K. (2018). Sedimentary record of Andean mountain building. *Earth-Science Reviews*, *178*, 279–309. https://doi.org/10.1016/j.earscirev.2017.11.025

Ichikawa, K., Miyata, T., & Shinohara, M. (1981). Eastward stepwise shift of the Izumi sedimentary basin with reference to the movement picture of the Median Tectonic Line. *Proceedings of the Kansai Branch*, *89*, 11–12.

Ichikawa, K., Shinohara, M., & Miyata, T. (1979). Stratigraphy of the Izumi Group in Izumi Mountains. *Proceedings of the Kansai Branch*, *85*, 10–11.

Ichiyama, Y., Ishiwatari, A., Kimura, J.-I., Senda, R., & Miyamoto, T. (2014). Jurassic plume-origin ophiolites in Japan: accreted fragments of oceanic plateaus. *Contributions to Mineralogy and Petrology*, *168*(1), 1019. https://doi.org/10.1007/s00410-014-1019-1

Igo, H. (1980). Geology in the Kanto Mountains. *Regional Geology of Japan," Kanto District". Asakura, Tokyo*, 2–74.

Ikeda, T., Harada, T., Kouchi, Y., Morita, S., Yokogawa, M., Yamamoto, K., & Otoh, S. (2016). Provenance analysis based on detritalzirconage spectra of the Lower Cretaceous formations in the Ryoseki-Monobe Area, outer zone of Southwest Japan. *Memoir of the Fukui Prefectural Dinosaur Museum*, *15*, 33–84.

Ingersoll, R. V. (1978). Paleogeography and paleotectonics of the late Mesozoic forearc basin of northern and central California. In D. G. Howell & K. A. McDougall (Eds.), *Mesozoic Paleogeography of the Western United States* (Vol. 2, pp. 471–482). Society of Economic Paleontologists and Mineralogists, Pacific Coast Paleogeography Symposium.

Isozaki, Y. (1988a). Permian, Triassic and Jurassic bedded radiolarian cherts in North Palawan Block, Philippines:Evidence of Late Mesozoic subduction-accretion. *Report No.2 of the IGCP Project 224:Pre-Jurassic Evolution of Eastern Asia*, 99–115. https://cir.nii.ac.jp/crid/1570291224313276288

Isozaki, Y. (1988b). Sanbagawa metamorphism and the formation of the Sanbosan-Shimanto belt. *Earth Monthly*, *10*, 367–371.

Isozaki, Y. (1996). Anatomy and genesis of a subduction-related orogen: A new view of geotectonic subdivision and evolution of the Japanese Islands. *The Island Arc*, *5*(3), 289–320. https://doi.org/10.1111/j.1440-1738.1996.tb00033.x

Isozaki, Y. (1997). Jurassic accretion tectonics of Japan. *The Island Arc*, *6*(1), 25–51. https://doi.org/10.1111/j.1440-1738.1997.tb00039.x

Isozaki, Y. (2000). The Japanese Islands: Its origin, evolution, and future. *Science Journal Kagaku*, *70*, 133–145.

Isozaki, Y., Aoki, K., Nakama, T., & Yanai, S. (2010). New insight into a subduction-related orogen: A reappraisal of the geotectonic framework and evolution of the Japanese Islands. *Gondwana Research*, *18*(1), 82–105. https://doi.org/https://doi.org/10.1016/j.gr.2010.02.015

Isozaki, Y., & Blake, M. C. (1994). Biostratigraphic constraints on formation and timing of accretion in a subduction complex: an example from the Franciscan Complex of northern California. *Journal of Geology*, *102*(3), 283–296. https://doi.org/10.1086/629671

Isozaki, Y., & Itaya, T. (1991). Pre-Jurassic klippe in northern Chichibu Belt in west-central Shikoku, Southwest Japan. Kurosegawa Terrane as a tectonic outlier of the pre-Jurassic rocks of the Inner

Zone. *The Journal of the Geological Society of Japan*, *97*(6), 431–450. https://doi.org/10.5575/geosoc.97.431

Isozaki, Y., Maruyama, S., & Furuoka, F. (1990). Accreted oceanic materials in Japan. *Tectonophysics*, *181*(1), 179–205. https://doi.org/https://doi.org/10.1016/0040-1951(90)90016-2

Ito, M., Aita, Y., & Hada, S. (2000). New radiolarian age information for the Chrystalls Beach Complex, southwest of Dunedin, New Zealand. *New Zealand Journal of Geology and Geophysics*, *43*(3), 349–354. https://doi.org/10.1080/00288306.2000.9514892

Ito, T., Kojima, Y., Kodaira, S., Sato, H., Kaneda, Y., Iwasaki, T., Kurashimo, E., Tsumura, N., Fujiwara, A., Miyauchi, T., Hirata, N., Harder, S., Miller, K., Murata, A., Yamakita, S., Onishi, M., Abe, S., Sato, T., & Ikawa, T. (2009). Crustal structure of southwest Japan, revealed by the integrated seismic experiment Southwest Japan 2002. *Tectonophysics*, *472*(1–4), 124–134. https://doi.org/10.1016/j.tecto.2008.05.013

Jackson, M. G., Becker, T. W., & Steinberger, B. (2021). Spatial Characteristics of Recycled and Primordial Reservoirs in the Deep Mantle. *Geochemistry, Geophysics, Geosystems*, *22*(3). https://doi.org/10.1029/2020GC009525

Jackson, M. G., & Macdonald, F. A. (2022). Hemispheric Geochemical Dichotomy of the Mantle Is a Legacy of Austral Supercontinent Assembly and Onset of Deep Continental Crust Subduction. *AGU Advances*, *3*(6), e2022AV000664. https://doi.org/10.1029/2022AV000664

Jasin, B., & Tongkul, F. (2013). Cretaceous radiolarians from Baliojong ophiolite sequence, Sabah, Malaysia. *Journal of Asian Earth Sciences*, *76*, 258–265. https://doi.org/10.1016/j.jseaes.2012.10.038

Jennings, W. L. (1991). The geochemistry of the Waipapa terrane metabasalts [Ph.D Thesis]. In *PhD thesis, University of Auckland*. University of Auckland.

Jones, D. L., Blake Jr., M. C., Rangin, C., & Geologists, A. A. of P. (1976). The four Jurassic belts of northern California and their significance to the geology of the southern California borderland. In D. G. Howell (Ed.), *Aspects of the geologic history of the California continental borderland* (pp. 343–362). American Association of Petroleum Geologists. http://pubs.er.usgs.gov/publication/70197659

Kanmera, K., & Sano, H. (1991). Collisional collapse and accretion of late Paleozoic Akiyoshi seamount. *Episodes Journal of International Geoscience*, *14*(3), 217–223. https://doi.org/10.18814/EPIIUGS/1991/V14I3/004

Kanmera, K., Sano, H., & Isozaki, Y. (1990). Akiyoshi terrane. In *Pre-Cretaceous Terranes of Japan* (pp. 49–62).

Kawamura, M. (1986). Constitution and occurrences of the Paleozoic and Mesozoic formations in SW Hokkaido, northern Japan. *Monogr. Assoc. Geol. Collab. Japan*, *31*, 17–32.

Kear, D., & Mortimer, N. (2003). Waipa Supergroup, New Zealand: A proposal. *Journal of the Royal Society of New Zealand*, *33*(1), 149–163. https://doi.org/10.1080/03014223.2003.9517725

Kennan, L., & Pindell, J. L. (2009). Dextral shear, terrane accretion and basin formation in the Northern Andes: best explained by interaction with a Pacific-derived Caribbean Plate?

Geological Society, London, Special Publications, *328*(1), 487–531. https://doi.org/10.1144/SP328.20

Khanchuk, A. I., Visotsky, S. V, & Panchenko, I. V. (1988). Correlation of metamorphic complexes of Shikote-Alin and Sakhalin. *Problems of Magmatism, Metamorphism and Mineralization of the Far East, Yuzhno-Sakhalinsk*.

Khogenkumar, S., Singh, A. K., Bikramaditya Singh, R. K., Khanna, P. P., Singh, N. I., & Singh, W. I. (2016). Coexistence of MORB and OIB-type mafic volcanics in the Manipur Ophiolite Complex, Indo-Myanmar Orogenic Belt, northeast India: Implication for heterogeneous mantle source at the spreading zone. *Journal of Asian Earth Sciences*, *116*, 42–58. https://doi.org/10.1016/j.jseaes.2015.11.007

Kienast, J.-R., & Rangin, C. (1982). Mesozoic blueschists and mélanges of Cedros Island (Baja California, Mexico): a consequence of nappe emplacement or subduction? *Earth and Planetary Science Letters*, *59*(1), 119–138. https://doi.org/10.1016/0012-821X(82)90121-2

Kilmer, F. H. (1977). Reconnaissance Geology of Cedros Island, Baja California, Mexico. *Bulletin, Southern California Academy of Sciences*, *76*, 91–98.

Kimbrough, D. L. (1982). *Structure, Petrology And Geochronology Of Mesozoic Paleooceanic Terranes On Cedros Island And The Vizcaino Peninsula, Baja California Sula, Mexico* [Ph.D Thesis]. University of California.

Kimbrough, D. L. (1989). *Franciscan Complex Rocks on Cedros Island, Baja California Sur, Mexico: Radiolarian Biostratigraphic Ages from a Chert Melange Block and Petrographic Observations on Metasandstone*.

Kimbrough, D. L., & Moore, T. E. (2003). Ophiolite and volcanic arc assemblages on the Vizcaino Peninsula and Cedros Island, Baja California Sur, México: Mesozoic forearc lithosphere of the Cordilleran magmatic arc. In *Tectonic evolution of northwestern Mexico and the Southwestern USA* (Vol. 374, pp. 43–71). Geological Society of America. https://doi.org/10.1130/0-8137-2374-4.43

Kiminami, K., Kawabata, K., & Miyashita, S. (1990). Discovery of Paleogene radiolarians from the Hidaka Supergroup and its significance with special reference to ridge subduction. *The Journal of the Geological Society of Japan*, *96*(4), 323–326. https://doi.org/10.5575/geosoc.96.323

Kimura, G. (1994). The latest Cretaceous-Early Paleogene rapid growth of accretionary complex and exhumation of high pressure series metamorphic rocks in northwestern Pacific margin. *Journal of Geophysical Research: Solid Earth*, *99*(B11), 22147–22164. https://doi.org/10.1029/94JB00959

Kimura, G. (1997). Cretaceous episodic growth of the Japanese Islands. *The Island Arc*, *6*(1), 52–68. https://doi.org/10.1111/j.1440-1738.1997.tb00040.x

Kimura, G., & Mukai, A. (1991). Underplated units in an accretionary complex: Melange of the Shimanto Belt of eastern Shikoku, southwest Japan. *Tectonics*, *10*(1), 31–50.

Kimura, G., Sakakibara, M., Ofuka, H., Ishizuka, H., Miyashita, S., Okamura, M., Melinikov, O. A., & Lushchenko, V. (1992). A deep section of accretionary complex: Susunai Complex in

Sakhalin Island, Northwest Pacific Margin. *The Island Arc*, *1*(1), 166–175. https://doi.org/10.1111/j.1440-1738.1992.tb00067.x

Kirschvink, J. L., Isozaki, Y., Shibuya, H., Otofuji, Y., Raub, T. D., Hilburn, I. A., Kasuya, T., Yokoyama, M., & Bonifacie, M. (2015). Challenging the sensitivity limits of Paleomagnetism: Magnetostratigraphy of weakly magnetized Guadalupian–Lopingian (Permian) Limestone from Kyushu, Japan. *Palaeogeography, Palaeoclimatology, Palaeoecology*, *418*, 75–89. https://doi.org/10.1016/j.palaeo.2014.10.037

Kobayashi, T., & Tamura, M. (1984a). The Triassic bivalvia of Malaysia, Thailand and adjacent areas. *Geology and Palaeontology of Southeast Asia*, *25*, 201–228.

Kobayashi, T., & Tamura, M. (1984b). The Triassic bivalvia of Malaysia, Thailand and adjacent areas. *Geology and Palaeontology of Southeast Asia*, 201–227.

Kodama, K., Fukuoka, M., Aita, Y., Sakai, T., Hori, R., Takemura, A., Campbell, H., Hollis, C., Grant-Mackie, J. A., & Spörli, K. B. (2007). Paleomagnetic Results from Arrow Rocks in the framework of Paleomagnetism in Pre-Neogene rocks from New Zealand. *GNS Science Monograph*, *24*, 177–196.

Koizumi, K., & Ishiwatari, A. (2006). Oceanic plateau accretion inferred from Late Paleozoic greenstones in the Jurassic Tamba accretionary complex, southwest Japan. *Island Arc*, *15*(1), 58–83. https://doi.org/10.1111/J.1440-1738.2006.00518.X

Konigsmark, T. (1998). *Geologic Trips: San Francisco & the Bay Area*. Geopress.

Kusky, T. M., & Bradley, D. C. (1999). Kinematic analysis of mélange fabrics: examples and applications from the McHugh Complex, Kenai Peninsula, Alaska. *Journal of Structural Geology*, *21*(12), 1773–1796. https://doi.org/10.1016/S0191-8141(99)00105-4

Kusky, T. M., Bradley, D. C., & Haeussler, P. (1997). Progressive deformation of the Chugach accretionary complex, Alaska, during a paleogene ridge-trench encounter. *Journal of Structural Geology*, *19*(2), 139–157. https://doi.org/10.1016/S0191-8141(96)00084-3

Kusky, T. M., Windley, B. F., Safonova, I., Wakita, K., Wakabayashi, J., Polat, A., & Santosh, M. (2013). Recognition of ocean plate stratigraphy in accretionary orogens through Earth history: A record of 3.8billion years of sea floor spreading, subduction, and accretion. *Gondwana Research*, *24*(2), 501–547. https://doi.org/https://doi.org/10.1016/j.gr.2013.01.004

Kusky, T. M., & Young, C. P. (1999). Emplacement of the Resurrection Peninsula ophiolite in the southern Alaska forearc during a ridge-trench encounter. *Journal of Geophysical Research: Solid Earth*, *104*(B12), 29025–29054. https://doi.org/10.1029/1999JB900265

Larson, R. L., & Chase, C. G. (1972). Late Mesozoic Evolution of the Western Pacific Ocean. *GSA Bulletin*, *83*(12), 3627–3644. https://doi.org/10.1130/0016-7606(1972)83[3627:LMEOTW]2.0.CO;2

Larson, R. L., & Pitman, W. C. (1972). World-Wide Correlation of Mesozoic Magnetic Anomalies, and Its Implications. *GSA Bulletin*, *83*(12), 3645–3662. https://doi.org/10.1130/0016-7606(1972)83[3645:WCOMMA]2.0.CO;2

Larue, D. K., Barnes, I., & Sedlock, R. L. (1989). Subduction and accretion of the permanente terrane near San Francisco, California. *Tectonics*, *8*(2), 221–235. https://doi.org/10.1029/TC008I002P00221

Li, X. (2018). The Mantle Plume Debates. *Open Journal of Yangtze Oil and Gas*, *03*(02), 147–152. https://doi.org/10.4236/ojogas.2018.32013

MacKinnon, T. C. (1983). Origin of the Torlesse terrane and coeval rocks, South Island, New Zealand. *Geological Society of America Bulletin*, *94*(8), 967–985.

Marquez, E. J., Aitchison, J. C., & Zamoras, L. R. (2006). Upper Permian to Middle Jurassic radiolarian assemblages of Busuanga and surrounding islands, Palawan, Philippines. *Eclogae Geologicae Helvetiae*, *99*(S1), S101–S125. https://doi.org/10.1007/s00015-006-0606-1

Maruyama, S., Isozaki, Y., Kimura, G., & Terabayashi, M. (1997a). Paleogeographic maps of the Japanese Islands: Plate tectonic synthesis from 750 Ma to the present. *The Island Arc*, *6*(1), 121–142. https://doi.org/10.1111/j.1440-1738.1997.tb00043.x

Maruyama, S., Isozaki, Y., Kimura, G., & Terabayashi, M. (1997b). Paleogeographic maps of the Japanese Islands: Plate tectonic synthesis from 750 Ma to the present. *Island Arc*, *6*(1), 121–142. https://doi.org/10.1111/J.1440-1738.1997.TB00043.X

Maruyama, S., & Seno, T. (1986). Orogeny and relative plate motions: Example of the Japanese Islands. *Tectonophysics*, *127*(3–4), 305–329. https://doi.org/10.1016/0040-1951(86)90067-3

Matsumoto, T. (1978). Japan and adjoining areas. In M. Moullade & A. Nairn (Eds.), *The Phanerozoic geology of the world II. Mesozoic, A* (pp. 79–144). Elsevier, Amsterdam.

Matsuoka, A. (1995). Jurassic and Lower Cretaceous radiolarian zonation in Japan and in the western Pacific. *Island Arc*, *4*(2), 140–153. https://doi.org/10.1111/J.1440-1738.1995.TB00138.X

Matsuoka, A., Yamakita, S., Sakakibara, M., & Hisada, K. (1998). Unit division for the Chichibu Composite Belt from a view point of accretionary tectonics and geology of western Shikoku, Japan. *The Journal of the Geological Society of Japan*, *104*(9), 634–653. https://doi.org/10.5575/geosoc.104.634

Meschede, M., & Frisch, W. (1994). Geochemical characteristics of basaltic rocks from the Central American ophiolites. *Profil*, *7*, 71–85.

Miyata, T. (1990). Slump strain indicative of paleoslope in Cretaceous Izumi sedimentary basin along Median tectonic line, southwest Japan. *Geology*, *18*(5), 392. https://doi.org/10.1130/0091-7613(1990)018<0392:SSIOPI>2.3.CO;2

Montes, C., Rodriguez-Corcho, A. F., Bayona, G., Hoyos, N., Zapata, S., & Cardona, A. (2019). Continental margin response to multiple arc-continent collisions: The northern Andes-Caribbean margin. *Earth-Science Reviews*, *198*, 102903. https://doi.org/10.1016/j.earscirev.2019.102903

Morgan, W. J. (1971). Convection Plumes in the Lower Mantle. *Nature*, *230*(5288), 42–43. https://doi.org/10.1038/230042a0

Mortimer, N., Rattenbury, M., King, P., Bland, K., Barrell, D., Bache, F., Begg, J., Campbell, H., Cox, S., Crampton, J., Edbrooke, S., Forsyth, P., Johnston, M., Jongens, R., Lee, J., Leonard, G.,

Raine, J., Skinner, D., Timm, C., … Turnbull, R. (2014). High-level stratigraphic scheme for New Zealand rocks. *New Zealand Journal of Geology and Geophysics*, *57*(4), 402–419. https://doi.org/10.1080/00288306.2014.946062

Müller, R. D., & Seton, M. (2015). Paleophysiography of Ocean Basins. In *Encyclopedia of Marine Geosciences* (pp. 1–15). Springer Netherlands. https://doi.org/10.1007/978-94-007-6644-0_84-1

Müller, R. D., Seton, M., Zahirovic, S., Williams, S. E., Matthews, K. J., Wright, N. M., Shephard, G. E., Maloney, K. T., Barnett-Moore, N., Hosseinpour, M., Bower, D. J., & Cannon, J. (2016). Ocean Basin Evolution and Global-Scale Plate Reorganization Events Since Pangea Breakup. *Annual Review of Earth and Planetary Sciences*, *44*(1), 107–138. https://doi.org/10.1146/annurev-earth-060115-012211

Murchey, B. L. (1984). Biostratigraphy and lithostratigraphy of chert in the Franciscan Complex, Marin Headlands, California. In M. C. J. Blake (Ed.), *Franciscan Geology of Northern California* (Vol. 43, pp. 51–70). Pacific Section, Society of Economic Paleontologists and Mineralogists.

Murchey, B. L., & Jones, D. L. (1984). Age and significance of chert in the Franciscan Complex in the San Francisco Bay Region. In C. M. J. Blake (Ed.), *Franciscan Geology of Northern California* (Vol. 43, pp. 23–40). Pacific Section of Economic Paleontologists and Mineralogists.

Nakae, S. (2000). Regional correlation of the Jurassic accretionary complex in the Inner Zone of Southwest Japan. *Memoirs of the Geological Society of Japan*, *55*, 73–98.

Nakagawa, M., Santosh, M., & Maruyama, S. (2009). Distribution and mineral assemblages of bedded manganese deposits in Shikoku, Southwest Japan: Implications for accretion tectonics. *Gondwana Research*, *16*(3–4), 609–621. https://doi.org/10.1016/J.GR.2009.05.003

Nakashima, K., & Sano, H. (2007). Palaeoenvironmental implication of resedimented limestones shed from Mississippian–Permian mid-oceanic atoll-type buildup into slope-to-basin facies, Akiyoshi, Japan. *Palaeogeography, Palaeoclimatology, Palaeoecology*, *247*(3–4), 329–356. https://doi.org/10.1016/j.palaeo.2006.11.004

Nelson, K. D. (1982). A suggestion for the origin of mesoscopic fabric in accretionary melange, based on features observed in the Chrystalls Beach Complex, South Island, New Zealand. *Geological Society of America Bulletin*, *93*(7), 625–634.

Nelson, S. W., & Blome, C. D. (1991). *Preliminary geochemistry of volcanic rocks from the McHugh Complex and Kachernak terrane, southern Alaska*.

Noda, A., & Sato, D. (2018). Submarine slope-fan sedimentation in an ancient forearc related to contemporaneous magmatism: The Upper Cretaceous Izumi Group, southwestern Japan. *Island Arc*, *27*(2), e12240. https://doi.org/10.1111/iar.12240

Noda, A., & Toshimitsu, S. (2009). Backward stacking of submarine channel–fan successions controlled by strike-slip faulting: The Izumi Group (Cretaceous), southwest Japan. *Lithosphere*, *1*(1), 41–59. https://doi.org/10.1130/L19.1

Nozaki, T., Nakamura, K., Osawa, H., Fujinaga, K., & Kato, Y. (2005). Geochemical Features and Tectonic Setting of Greenstones from Kunimiyama, Northern Chichibu Belt, Central Shikoku, Japan. *Resource Geology*, *55*(4), 301–310. https://doi.org/10.1111/j.1751-3928.2005.tb00252.x

Oda, H., & Suzuki, H. (2000). Paleomagnetism of Triassic and Jurassic red bedded chert of the Inuyama area, central Japan. *Journal of Geophysical Research: Solid Earth*, *105*(B11), 25743–25767. https://doi.org/10.1029/2000JB900267

Okada, A. (1973). QUATERNARY FAULTING ALONG THE MEDIAN TECTONIC LINE IN THE CENTRAL PART OF SHIKOKU. *Geographical Review of Japan*, *46*(5), 295–322. https://doi.org/10.4157/grj.46.295

Okamura, Y. (1991). Large-Scale Melange Formation Due to Seamount Subduction: An Example from the Mesozoic Accretionary Complex in Central Japan. *The Journal of Geology*, *99*(5), 661–674. https://doi.org/10.1086/629531

Onoue, T., Nagai, K., Kamishima, A., Seno, M., & Sano, H. (2004). Origin of basalts from Sambosan accretionary complex, Shikoku and Kyushu. *The Journal of the Geological Society of Japan*, *110*(4), 222–236. https://doi.org/10.5575/geosoc.110.222

Ozawa, H., Murata, M., & Itaya, T. (1997). Early Jurassic Volcanism of the Mikabu belt:Evidence from K-Ar age of picritic basalt, Kurouchi ultramafic mass, Kanto Mountains, Japan. *The Journal of the Geological Society of Japan*, *103*(11), 1089–1092. https://doi.org/10.5575/GEOSOC.103.1089

Ozawa, H., Murata, M., Nishimura, H., & Itaya, T. (1997). Petrological Feature and Dating of Igneous Rocks of the Mikabu Belt. *Bulletin of the Volcanological Society of Japan*, *42*, S231–S237. https://doi.org/10.18940/kazan.42.Special_S231

Pasco, J. A., Dycoco, J. M. A., Valera, G. T. V., Payot, B. D., Pillejera, J. D. B., Uy, F. A. A. E., Armada, L. T., & Dimalanta, C. B. (2019). Petrogenesis of ultramafic-mafic clasts in the Dos Hermanos Mélange, Ilocos Norte: Insights to the evolution of western Luzon, Philippines. *Journal of Asian Earth Sciences*, *184*, 104004. https://doi.org/10.1016/j.jseaes.2019.104004

Pindell, J. L., & Kennan, L. (2009). Tectonic evolution of the Gulf of Mexico, Caribbean and northern South America in the mantle reference frame: an update. *Geological Society, London, Special Publications*, *328*(1), 1–55. https://doi.org/10.1144/SP328.1

Queaño, K. L., Dimalanta, C. B., Yumul, G. P., Marquez, E. J., Faustino-Eslava, D. V., Suzuki, S., & Ishida, K. (2017). Stratigraphic units overlying the Zambales Ophiolite Complex (ZOC) in Luzon, (Philippines): Tectonostratigraphic significance and regional implications. *Journal of Asian Earth Sciences*, *142*, 20–31. https://doi.org/10.1016/j.jseaes.2016.06.011

Queaño, K. L., Marquez, E. J., Dimalanta, C. B., Aitchison, J. C., Ali, J. R., & Yumul, G. P. (2017). Mesozoic radiolarian faunas from the northwest Ilocos Region, Luzon, Philippines and their tectonic significance. *Island Arc*, *26*(4), e12195. https://doi.org/10.1111/iar.12195

Rangin, C. (1978). Speculative Model of Mesozoic Geodynamics, Central Baja California to Northeastern Sonora (Mexico). In Howell D.G. & Macdougall K.A. (Eds.), *Society of Economic Paleontologists and Mineralogists Mesozoic Symposium* (pp. 85–106).

Rangin, C. (1991). The Philippine Mobile Belt: a complex plate boundary. *Journal of Southeast Asian Earth Sciences*, *6*(3–4), 209–220. https://doi.org/10.1016/0743-9547(91)90068-9

Rangin, C., Girard, D., & Maury, R. (1983). Geodynamic significance of Late Triassic to Early Cretaceous volcanic sequences of Vizcaino Peninsula and Cedros Island, Baja California, Mexico. *Geology*, *11*(9), 552. https://doi.org/10.1130/0091-7613(1983)11<552:GSOLTT>2.0.CO;2

Rangin, C., Steinberg, M., & Bonnot-Courtois, C. (1981). Geochemistry of the Mesozoic bedded cherts of Central Baja California (Vizcaino-Cedros-San Benito): implications for paleogeographic reconstruction of an old oceanic basin. *Earth and Planetary Science Letters*, *54*(2), 313–322. https://doi.org/10.1016/0012-821X(81)90014-5

Rangin, C., Stephan, J. F., Butterlin, J., Bellon, H., Muller, C., Chorowicz, J., & Baladad, D. (1991). Collision neogene d'arc volcaniques dans le centre des Philippines; stratigraphie et structure de la chaine d'Antique (ile de Panay). *Bulletin de La Société Géologique de France*, *162*(3), 465–477. https://doi.org/10.2113/gssgfbull.162.3.465

Rikhter, A. V. (1981). Block structure of the Susunai range (southern Sakhalin). *Geotectonics*, *15*, 162–167.

Safonova, I., Kojima, S., Nakae, S., Romer, R. L., Seltmann, R., Sano, H., & Onoue, T. (2015). Oceanic island basalts in accretionary complexes of SW Japan: Tectonic and petrogenetic implications. *Journal of Asian Earth Sciences*, *113*, 508–523. https://doi.org/10.1016/j.jseaes.2014.09.015

Safonova, I., Litasov, K., & Maruyama, S. (2015). Triggers and sources of volatile-bearing plumes in the mantle transition zone. *Geoscience Frontiers*, *6*(5), 679–685. https://doi.org/10.1016/j.gsf.2014.11.004

Safonova, I., Maruyama, S., Kojima, S., Komiya, T., Krivonogov, S., & Koshida, K. (2016). Recognizing OIB and MORB in accretionary complexes: A new approach based on ocean plate stratigraphy, petrology and geochemistry. *Gondwana Research*, *33*, 92–114. https://doi.org/10.1016/j.gr.2015.06.013

Safonova, I., & Santosh, M. (2014). Accretionary complexes in the Asia-Pacific region: Tracing archives of ocean plate stratigraphy and tracking mantle plumes. *Gondwana Research*, *25*(1), 126–158. https://doi.org/10.1016/j.gr.2012.10.008

Safonova, I., Utsunomiya, A., Kojima, S., Nakae, S., Tomurtogoo, O., Filippov, A. N., & Koizumi, K. (2009). Pacific superplume-related oceanic basalts hosted by accretionary complexes of Central Asia, Russian Far East and Japan. *Gondwana Research*, *16*(3–4), 587–608. https://doi.org/10.1016/j.gr.2009.02.008

Saito, T., Okada, Y., Fujisaki, W., Sawaki, Y., Sakata, S., Dohm, J., Maruyama, S., & Hirata, T. (2014). Accreted Kula plate fragment at 94Ma in the Yokonami-melange, Shimanto-belt, Shikoku, Japan. *Tectonophysics*, *623*, 136–146. https://doi.org/10.1016/j.tecto.2014.03.026

Sakakibara, M., & Ota, T. (1994). Metamorphic evolution of the Kamuikotan high-pressure and low-temperature metamorphic rocks in central Hokkaido, Japan. *Journal of Geophysical Research: Solid Earth*, *99*(B11), 22221–22235. https://doi.org/10.1029/94JB00958

Sakakibara, M., Sakai, T., Hori, R. S., Spörli, B., Fujiki, T., Aida, Y., Takemura, A., Campbell, H., Takemura, S., Kamata, Y., Yamakita, S., Suzuki, N., Nakamura, Y., & Kodama, K. (2003). Basaltic sheet intruding into Middle-Late Permian pelagic sedimentary rocks at Arrow Rocks, Waipapa Terrane, North Island, New Zealand. *The Journal of the Geological Society of Japan*, *109*(12), XXIII–XXIV. https://doi.org/10.5575/geosoc.109.XXIII

Sakashima, T., Terada, K., Takeshita, T., & Sano, Y. (2003). Large-scale displacement along the Median Tectonic Line, Japan: evidence from SHRIMP zircon U–Pb dating of granites and gneisses from the South Kitakami and paleo-Ryoke belts. *Journal of Asian Earth Sciences*, *21*(9), 1019–1039. https://doi.org/10.1016/S1367-9120(02)00108-6

Sano, H. (1988a). Permian oceanic-rocks of Mino Terrane, central Japan Part I. Chert Facies. *The Journal of the Geological Society of Japan*, *94*(9), 697-709_2. https://doi.org/10.5575/geosoc.94.697

Sano, H. (1988b). Permian oceanic-rocks of Mino Terrane, central Japan Part II. Limestone facies. *Journal - Geological Society of Japan*, *94*(12), 963–976. https://doi.org/10.5575/GEOSOC.94.963

Sano, H. (2006). Impact of long-term climate change and sea-level fluctuation on Mississippian to Permian mid-oceanic atoll sedimentation (Akiyoshi Limestone Group, Japan). *Palaeogeography, Palaeoclimatology, Palaeoecology*, *236*(3–4), 169–189. https://doi.org/10.1016/j.palaeo.2005.11.009

Sano, H., Iijima, Y., & Hattori, H. (1987). Stratigraphy of the Paleozoic rocks in the Akiyoshi Terrane of the central Chugoku Massif. *Journal of the Geological Society of Japan*, *93*, 865–880.

Sano, H., & Kanmera, K. (1988). Paleogeographic reconstruction of accreted oceanic rocks, Akiyoshi, southwest Japan. *Geology*, *16*(7), 600. https://doi.org/10.1130/0091-7613(1988)016<0600:PROAOR>2.3.CO;2

Sano, H., & Kojima, S. (2000). Carboniferous to Jurassic oceanic rocks of Mino-Tamba-Ashio terrane. *Memoirs of the Geological Society of Japan*, *55*, 123–144. https://cir.nii.ac.jp/crid/1572543025677719936

Sano, S., Hayasaka, Y., & Tazaki, K. (2000). Geochemical characteristics of Carboniferous greenstones in the Inner Zone of Southwest Japan. *Island Arc*, *9*(1), 81–96. https://doi.org/10.1046/J.1440-1738.2000.00263.X

Sato, H., Kato, N., Abe, S., Van Horne, A., & Takeda, T. (2015). Reactivation of an old plate interface as a strike-slip fault in a slip-partitioned system: Median Tectonic Line, SW Japan. *Tectonophysics*, *644–645*, 58–67. https://doi.org/10.1016/j.tecto.2014.12.020

Sato, H., Kojima, Y., Murata, A., Ito, T., Kaneda, Y., Onishi, M., Iwasaki, T., Oho, Y., Ogino, S., & Kano, K. (2005). Crustal structure of the outer zone in southwest Japan revealed by Shikoku and Seto-Inland-Sea seismic profiling in 2002. *Bulletin of the Earthquake Research Institute*, *80*(2), 53–71.

Sato, T. (1962). Études biostratigraphiques des ammonites du Jurassique du Japon. *Mémoires de La Societé Géologique de France NS*, *94*, 1–122.

Sawada, H., Isozaki, Y., Aoki, S., Sakata, S., Sawaki, Y., Hasegawa, R., & Nakamura, Y. (2019). The Late Jurassic magmatic protoliths of the Mikabu greenstones in SW Japan: A fragment of an oceanic plateau in the Paleo-Pacific Ocean. *Journal of Asian Earth Sciences*, *169*, 228–236. https://doi.org/10.1016/J.JSEAES.2018.08.018

Schnur, S. R., & Gilbert, L. A. (2012). Detailed volcanostratigraphy of an accreted seamount: Implications for intraplate seamount formation. *Geochemistry, Geophysics, Geosystems*, *13*(12). https://doi.org/10.1029/2012GC004301

Sedlock, R. L. (1988). Tectonic setting of blueschist and island-arc terranes of west-central Baja California, Mexico. *Geology*, *16*(7), 623–626. https://doi.org/10.1130/0091-7613(1988)016<0623:TSOBAI>2.3.CO;2

Sedlock, R. L., & Isozaki, Y. (1990). Lithology and biostratigraphy of Franciscan-like chert and associated rocks in west-central Baja California, Mexico. *Geological Society of America Bulletin*, *102*(7), 852–864. https://doi.org/10.1130/0016-7606(1990)102<0852:LABOFL>2.3.CO;2

Seton, M., Müller, R. D., Zahirovic, S., Gaina, C., Torsvik, T., Shephard, G., Talsma, A., Gurnis, M., Turner, M., Maus, S., & Chandler, M. (2012). Global continental and ocean basin reconstructions since 200Ma. *Earth-Science Reviews*, *113*(3–4), 212–270. https://doi.org/10.1016/j.earscirev.2012.03.002

Seton, M., Müller, R. D., Zahirovic, S., Williams, S., Wright, N. M., Cannon, J., Whittaker, J. M., Matthews, K. J., & McGirr, R. (2020). A Global Data Set of Present-Day Oceanic Crustal Age and Seafloor Spreading Parameters. *Geochemistry, Geophysics, Geosystems*, *21*(10). https://doi.org/10.1029/2020GC009214

Shibuya, H., & Sasajima, S. (1986a). Paleomagnetism of red cherts: A case study in the Inuyama Area, central Japan. *Journal of Geophysical Research: Solid Earth*, *91*(B14), 14105–14116. https://doi.org/10.1029/JB091iB14p14105

Shibuya, H., & Sasajima, S. (1986b). Paleomagnetism of red cherts: A case study in the Inuyama Area, central Japan. *Journal of Geophysical Research: Solid Earth*, *91*(B14), 14105–14116. https://doi.org/10.1029/JB091iB14p14105

Sliter, W. V. (1984). Foraminifers from Cretaceous limestone of the Franciscan Complex, northern California. In C. M. J. Blake (Ed.), *Franciscan Geology of Northern California* (Vol. 43, pp. 149–162). Pacific Section of Economic Paleontologists and Mineralogists.

Spörli, K. B. (1978). Mesozoic tectonics, North Island, New Zealand. *Geological Society of America Bulletin*, *89*(3), 415–425.

Spörli, K. B., Aita, Y., & Gibson, G. W. (1989). Juxtaposition of Tethyan and non-Tethyan Mesozoic radiolarian faunas in melanges, Waipapa terrane, North Island, New Zealand. *Geology*, *17*(8), 753–756. https://doi.org/10.1130/0091-7613(1989)017<0753:JOTANT>2.3.CO;2

Spörli, K. B., & Grant-Mackie, J. A. (1976). Upper jurassic fossils from the Waipapa group of Tawharanui Peninsula, North Auckland, New Zealand. *New Zealand Journal of Geology and Geophysics*, *19*(1), 21–34. https://doi.org/10.1080/00288306.1976.10423547

Stern, R. J. (2007). When and how did plate tectonics begin? Theoretical and empirical considerations. *Chinese Science Bulletin*, *52*(5), 578–591. https://doi.org/10.1007/s11434-007-0073-8

Sugiyama, Y. (1994). Neotectonics of Southwest Japan due to the right-oblique subduction of the Philippine Sea plate. *Geofísica Internacional*, *33*(1), 53–76. https://doi.org/10.22201/igeof.00167169p.1994.33.1.540

Taira, A., Katto, J., Tahiro, M., Okamura, M., & Kodama, M. (1988). The Shimanto belt in Shikoku, Japan-evolution of Cretaceous to Miocene accretionary prism. *Modern Geology*, *12*, 5–46.

Taira, A., Okada, H., Whitaker, J. H., & Smith, A. J. (1982). The Shimanto Belt of Japan: Cretaceous-lower Miocene active-margin sedimentation. *Geological Society, London, Special Publications*, *10*(1), 5–26. https://doi.org/10.1144/GSL.SP.1982.010.01.01

Taira, A., Saito, Y., & Hashimoto, M. (1983). The role of oblique subduction and strike-slip tectonics in the evolution of Japan. In T. W. C. Hilde & S. Uyeda (Eds.), *Geodynamics of the Western Pacific-Indonesian Region* (Vol. 11, pp. 303–316). https://doi.org/10.1029/GD011p0303

Takemura, A., Aita, Y., Hori, R. S., Higuchi, Y., Spörli, K. B., Campbell, H. J., Kodama, K., & Sakai, T. (2002). Triassic radiolarians from the ocean-floor sequence of the Waipapa Terrane at Arrow Rocks, Northland, New Zealand. *New Zealand Journal of Geology and Geophysics*, *45*(3), 289–296. https://doi.org/10.1080/00288306.2002.9514974

Tamayo, R. A., Yumul, G. P., Maury, R. C., Polve, M., Cotten, J., & Bohn, M. (2001). Petrochemical Investigation of the Antique Ophiolite (Philippines): Implications on Volcanogenic Massive Sulfide and Podiform Chromitite Deposits. *Resource Geology*, *51*(2), 145–164. https://doi.org/10.1111/j.1751-3928.2001.tb00088.x

Tazawa, J.-I. (2002). Late Paleozoic brachiopod faunas of the South Kitakami Belt, northeast Japan, and their paleobiogeographic and tectonic implications. *The Island Arc*, *11*(4), 287–301. https://doi.org/10.1046/j.1440-1738.2002.00369.x

Tominaga, K., & Hara, H. (2021). Paleogeography of Late Jurassic large-igneous-province activity in the Paleo-Pacific Ocean: Constraints from the Mikabu greenstones and Chichibu accretionary complex, Kanto Mountains, Central Japan. *Gondwana Research*, *89*, 177–192. https://doi.org/10.1016/j.gr.2020.10.003

Tominaga, K., Hara, H., & Tokiwa, T. (2019). Zircon U–Pb ages of the Kashiwagi Unit of the accretionary complex in the Northern Chichibu Belt, Kanto Mountains, central Japan. *BULLETIN OF THE GEOLOGICAL SURVEY OF JAPAN*, *70*(3), 299–314. https://doi.org/10.9795/bullgsj.70.299

Torsvik, T. H., Steinberger, B., Gurnis, M., & Gaina, C. (2010). Plate tectonics and net lithosphere rotation over the past 150 My. *Earth and Planetary Science Letters*, *291*(1–4), 106–112. https://doi.org/10.1016/j.epsl.2009.12.055

Tournon, J., & Alvarado, G. (1997). Mapa Geológico de Costa Rica. Scale 1:500 000. *Cartago-Costa Rica. Editorial Tecnológica de Costa Rica*.

Ueda, H. (2003). Accretionary complex of remnant-arc origin: Greenstone-conglomerate-chert succession in the Oku-Niikappu area of the Idonnappu Zone, Hokkaido, Japan. *The Journal of the Geological Society of Japan*, *109*(9), XVII–XVIII. https://doi.org/10.5575/geosoc.109.XVII

Ueda, H., & Miyashita, S. (2003). Discovery of sheeted dikes in the Cretaceous accretionary complex of the Idonnappu Zone, Hokkaido, Japan. *The Journal of the Geological Society of Japan*, *109*(9), 559–562. https://doi.org/10.5575/GEOSOC.109.559

Ueda, H., & Miyashita, S. (2005). Tectonic accretion of a subducted intraoceanic remnant arc in Cretaceous Hokkaido, Japan, and implications for evolution of the Pacific northwest. *Island Arc*, *14*(4), 582–598. https://doi.org/10.1111/J.1440-1738.2005.00486.X

Uno, K., Furukawa, K., & Hada, S. (2011). Margin-parallel translation in the western Pacific: Paleomagnetic evidence from an allochthonous terrane in Japan. *Earth and Planetary Science Letters*, *303*(1–2), 153–161. https://doi.org/10.1016/j.epsl.2011.01.002

van Hinsbergen, D. J. J., & Schouten, T. L. A. (2021). Deciphering paleogeography from orogenic architecture: Constructing orogens in a future supercontinent as thought experiment. *American Journal of Science*, *321*(6), 955–1031. https://doi.org/10.2475/06.2021.09

van Hinsbergen, D. J. J., Torsvik, T. H., Schmid, S. M., Maţenco, L. C., Maffione, M., Vissers, R. L. M., Gürer, D., & Spakman, W. (2020). Orogenic architecture of the Mediterranean region and kinematic reconstruction of its tectonic evolution since the Triassic. *Gondwana Research*, *81*, 79–229. https://doi.org/10.1016/J.GR.2019.07.009

Wahrhaftig, C. (1984). Structure of the Marin Headlands block, California: A progress report. In M. C. J. Blake (Ed.), *Franciscan Geology of Northern California* (Vol. 43, pp. 31–50). Pacific Section of Economic Paleontologists and Mineralogists.

Wakabayashi, J. (1992). Nappes, Tectonics of Oblique Plate Convergence, and Metamorphic Evolution Related to 140 Million Years of Continuous Subduction, Franciscan Complex, California. *The Journal of Geology*, *100*(1), 19–40. https://doi.org/10.1086/629569

Wakabayashi, J. (2011). Mélanges of the Franciscan Complex, California: Diverse structural settings, evidence for sedimentary mixing, and their connection to subduction processes. In *Mélanges: Processes of Formation and Societal Significance*. Geological Society of America. https://doi.org/10.1130/2011.2480(05)

Wakabayashi, J. (2015). Anatomy of a subduction complex: architecture of the Franciscan Complex, California, at multiple length and time scales. *International Geology Review*, *57*(5–8), 669–746. https://doi.org/10.1080/00206814.2014.998728

Wakabayashi, J. (2017). Structural context and variation of ocean plate stratigraphy, Franciscan Complex, California: insight into mélange origins and subduction-accretion processes. *Progress in Earth and Planetary Science*, *4*(1), 18. https://doi.org/10.1186/s40645-017-0132-y

Wakabayashi, J., Ghatak, A., & Basu, A. R. (2010). Suprasubduction-zone ophiolite generation, emplacement, and initiation of subduction: A perspective from geochemistry, metamorphism, geochronology, and regional geology. *Geological Society of America Bulletin*, *122*(9–10), 1548–1568. https://doi.org/10.1130/B30017.1

Wakita, K. (2012). Mappable features of mélanges derived from Ocean Plate Stratigraphy in the Jurassic accretionary complexes of Mino and Chichibu terranes in Southwest Japan. *Tectonophysics*, *568–569*, 74–85. https://doi.org/10.1016/j.tecto.2011.10.019

Wakita, K., & Metcalfe, I. (2005). Ocean Plate Stratigraphy in East and Southeast Asia. *Journal of Asian Earth Sciences*, *24*(6), 679–702. https://doi.org/10.1016/j.jseaes.2004.04.004

Wandres, A. M., & Bradshaw, J. D. (2005). New Zealand tectonostratigraphy and implications from conglomeratic rocks for the configuration of the SW Pacific margin of Gondwana. *Geological Society, London, Special Publications*, *246*(1), 179–216. https://doi.org/10.1144/GSL.SP.2005.246.01.06

Wandres, A. M., Bradshaw, J. D., & Ireland, T. (2005). The Paleozoic-Mesozoic recycling of the Rakaia Terrane, South Island, New Zealand: Sandstone clast and sandstone petrology, geochemistry, and geochronology. *New Zealand Journal of Geology and Geophysics*, *48*(2), 229–245. https://doi.org/10.1080/00288306.2005.9515112

Yamakita, S., & Otoh, S. (2000). Estimation of the amount of Late Cretaceous left-lateral strike-slip displacement along the Median Tectonic Line and its implications in the juxtaposition of some geological belts of Southwest Japan. *Association for the Geological Collaboration in Japan Monograph*, *49*, 93–104.

Yamamoto, K. (1987). Geochemical characteristics and depositional environments of cherts and associated rocks in the Franciscan and Shimanto Terranes. *Sedimentary Geology*, *52*(1–2), 65–108. https://doi.org/10.1016/0037-0738(87)90017-0

Yao, A. (2000). Terrane arrangement of Southwest Japan in view of the Paleozoic-Mesozoic tectonics of East Asia. Assoc Geol Collab Japan. *Monograph*, *49*, 145–155.

Yegorov, A. E. (1967). New data on the ages of metamorphic complexes in Sakhalin Island. *Doklady Nauk USSR*, *175*, 2–15.

Young, A., Flament, N., Maloney, K., Williams, S., Matthews, K., Zahirovic, S., & Müller, R. D. (2019). Global kinematics of tectonic plates and subduction zones since the late Paleozoic Era. *Geoscience Frontiers*, *10*(3), 989–1013. https://doi.org/10.1016/j.gsf.2018.05.011

Yumul, G. P., Dimalanta, C. B., Faustino, D. V., & De Jesus, J. V. (1998). Translation and docking of an arc terrane: geological and geochemical evidence from the southern Zambales Ophiolite Complex, Philippines. *Tectonophysics*, *293*(3–4), 255–272. https://doi.org/10.1016/S0040-1951(98)00096-1

Yumul, G. P., Dimalanta, C. B., Gabo-Ratio, J. A. S., Queaño, K. L., Armada, L. T., Padrones, J. T., Faustino-Eslava, D. V., Payot, B. D., & Marquez, E. J. (2020). Mesozoic rock suites along western Philippines: Exposed proto-South China Sea fragments? *Journal of Asian Earth Sciences: X*, *4*, 100031. https://doi.org/10.1016/j.jaesx.2020.100031

Yumul, G. P., Dimalanta, C. B., Salapare, R. C., Queaño, K. L., Faustino-Eslava, D. V., Marquez, E. J., Ramos, N. T., Payot, B. D., Guotana, J. M. R., Gabo-Ratio, J. A. S., Armada, L. T., Padrones, J. T., Ishida, K., & Suzuki, S. (2020). Slab rollback and microcontinent subduction in the evolution of the Zambales Ophiolite Complex (Philippines): A review. *Geoscience Frontiers*, *11*(1), 23–36. https://doi.org/10.1016/j.gsf.2018.12.008

Zamoras, L. R., & Matsuoka, A. (2001). Malampaya Sound Group : a Jurassic-Early Cretaceous accretionary complex in Busuanga Island, North Palawan Block (Philippines). *Journal of the Geological Society of Japan*, *107*(5), 316–336. https://doi.org/10.5575/GEOSOC.107.316

Zamoras, L. R., & Matsuoka, A. (2004). Accretion and postaccretion tectonics of the Calamian Islands, North Palawan block, Philippines. *The Island Arc*, *13*(4), 506–519. https://doi.org/10.1111/j.1440-1738.2004.00443.x

Zharov, A. E. (2005). South Sakhalin tectonics and geodynamics: A model for the Cretaceous-Paleogene accretion of the East Asian continental margin. *Russian Journal of Earth Sciences*, *7*(5). https://doi.org/10.2205/2005ES000190

Appendix

Table 1. Database of the accreted OPS for the Circum Pacific

Acc. Comp.	Site	Birth of Oceanic Plate	Age of Accretion	Affinity	Volc. Rock Type	Lat.	Long.	Ref.
Izanagi Plates								
Russia								
Susunai Complex	Okhotsk Sea coastline (Kema River)	Late Triassic (Norian ~220 Ma)	55 Ma	T or N-MORB	Basalt, Pillow Basalt	47.279	142.967	[20]
	Okhotsk Sea coastline (Anna River)	Late Triassic (Norian ~220 Ma)	55 Ma	OIB	Dolerite	47.175	143.000	[20]
Japan								
Akiyoshi	Akiyoshi-dai (Edo, Yamaguci Area)	Early Carboniferous- upper Visean	Late Permian (lower Wuchiapingian)	OIB	Aphyric Basalt	34.279	131.348	[2, 5]
	Taishaku-dai	Early Carboniferous- upper Visean	Late Permian (lower Wuchiapingian)	OIB	Aphyric Basalt	34.854	133.245	[4, 11]
	Atetsu-dai	Early Carboniferous- upper Visean	Late Permian (lower Wuchiapingian)	OIB	Aphyric Basalt	34.736	133.490	[4, 11]
Mino-Tamba-Ashio	Haciman (Nagara River)	>Mid triassic	Early Cretaceous (Berriasian)	OIB	Dolerite	35.696	136.950	[2, 10]
	Neo (Neohigashidagawa River)	early Permian	Early Cretaceous (Berriasian)	OIB	Diabase, Dolerite	35.710	136.669	[2, 11]
	Kiso River (Inuyama)	Trassic	Late Jurassic	MORB	Basalt	35.422	136.973	[2, 11]
	Tsurube (Shuzan Complex-)	Early-Middle Permian	Early Cretaceous (Berriasian)	OIB, MORB	Dolerite	35.547	135.827	[1, 10]
	Somegaya River (North Tamba)	Late Carboniferous (330-340 Ma)	Early Cretaceous (Berriasian)	OIB, NMORB	Basalt	35.372	135.640	[12]
	Kiyoki River (South Tamba)	Late Carboniferous (330-340 Ma)	Early Cretaceous (Berriasian)	OIB	Basalt	35.122	135.673	[12]
Sothern Chichibu	Kumagawa River (Sambosan Unit)	earlies Late Triassic	Early Cretaceous (Berriasian)	OIB	Porphyric Basalt	32.293	130.602	[2, 6]
Northern Chichibu	Kawanokawa Mine (Sumaizuku Unit)	Late Carboniferous	Middle Jurassic	OIB	Porphyric Basalt	33.674	133.696	[2, 7]

Acc. Comp.	Site	Birth of Oceanic Plate	Age of Accretion	Affinity	Volc. Rock Type	Lat.	Long.	Ref.
	Kunimiyama mine (Sumaizuku Unit)	Late Carboniferous	Middle Jurassic	OIB, (E-)MORB	Porphyric Basalt	33.629	133.550	2, 7
	Kanto Mountain (Kashiwagi Unit)	Middle Triassic	Early Cretaceous	OIB	Diabase	36.204	138.850	2, 7, 52, 53
	Kanto Mountain (Kashiwagi Unit)	Middle Triassic	Early Cretaceous	OPB	Basalt	36.204	138.850	52, 53
	Kanto Mountain (Kamiyoshida unit)	Late Carboniferous	Middle Jurassic	OIB	Basalt	36.204	138.850	52, 53
Mikabu Greenstones	Toba Complex	Late Jurassic (Kimmeridgian - 154.6 Ma)	Early Cretaceous (Berriasian)	N-MORB	Basalt	34.462	136.761	2, 3, 8, 13
	Toba Complex	Late Jurassic (Kimmeridgian - 154.6 Ma)	Early Cretaceous (Berriasian)	OPB	Gabbro/ Diabase	34.462	136.761	3, 8, 9, 13
	Asama Mountain	Late Permian	Early Cretaceous (Berriasian)	OIB	Mikabu Gabbro	34.458	136.780	3, 8, 9
	Kanto Mountain	earlies Early Triassic (Hettagian - 199.4 Ma)	Early Cretaceous (Berriasian)	N-MORB	Picritic Basalt	36.204	138.850	3, 8, 14
	Kanto Mountain	Late Jurassic (Kimmeridgian - 157 ± 0.9 Ma)	Early Cretaceous (Berriasian)	OIB	Basalt	36.204	138.850	52, 53
Shimanto	Shikoku (Sumiyoshi Beach)	Early Cretaceous	Late Cretaceous (Cenomanian)	OIB	Pillow Lava (Diabase and Dolerite)	33.520	133.761	2, 18
	Kii Peninsula	??	Late Cretaceous (Campanian - Maastrichtian)	OFB	Pillow Lava	?	?	17
Sorachi-Yezo Belt	Shizunai River	??	early Cretaceous (Valanginian - 135 Ma) - Aptian	OIB	Alkaline Pillow Basalt	42.415	142.565	16
	Oku-Niikappu (Niikappu River)	Late Jurassic (Thitonian) /earliest Early Cretaceous (Berriasian)	late Early Cretaceous- Late Cretaceous (Albian-Cenomian)	MORB	Basalt (Dike)	42.581	142.544	19
Philippines								
Busuanga Acs	Calamian Island (Bicatan Melange)	Middle - Late Triassic (??? Or earlier)	early Cretaceous (Berriasian)	OIB (??)	??? Pillow Basalt	12.203	120.221	43, 44

Acc. Comp.	Site	Birth of Oceanic Plate	Age of Accretion	Affinity	Volc. Rock Type	Lat.	Long.	Ref.
Zambales	Acoje Block	Late Triassic	Early Cretaceous - early Miocene	MORB - IAT	Cummulate Troctolite-Gabbro	15.717	119.968	[45, 46]
Dos Hemanos	Dos Hermanos Melange	Late Jurrasic	Early Cretaceous - early Miocene	MORB - IAT	Cummulate Troctolite-Gabbro	18.503	120.737	[45, 48]
Panay Peninsula Acs	Paniciun Melange	Early Cretaceous	Middle Miocene	(T-) MORB, IAT	??	10.758	122.104	[45, 49]
Faralon Plates								
Costa Rica								
Santa Rosa AC	Sitio Santa Rosa (Santa Rosa AC)	older than Sinemurian	late Early Cretaceous (~100 Ma)	OIB	Pillow Basalt	10.895	-85.907	[32]
	Sitio Santa Rosa (Santa Rosa AC)	Early Jurassic (Toarcian ~175 Ma)	late Early Cretaceous (~100 Ma)	OIB	Basalt Sill	10.881	-85.877	[29, 30, 31, 32]
Mexico								
Baja California	Cedros Island (Melange Complex)	Late Triassic (Lates Carniar to Middle Norian)	Albian (~105)	MORB	Pillow Basalt	28.097	-115.322	[34]
	Cedros Island (Melange Complex)	Late Triassic (Lates Carniar to Middle Norian)	Albian (~105)	MORB	Pillow Basalt	28.153	-115.322	[34]
	Cedros Island (Melange Complex)	Late Triassic (Lates Carniar to Middle Norian)	Albian (~105)	MORB	Pillow Basalt	28.042	-115.241	[34]
	Northern Vizcaino Peninsulsa (Ophiolite Complex)	Late Triassic (Norian 225 Ma)	Albian (~105)	MORB	Pillow Basalt	27.771	-114.978	[34]
	Poerto Nuevo Melange	Late Triassic (Norian 221 ± 2 Ma)	Albian (~105)	OIB	Gabbro Dike	27.504	-114.575	[34]
	Southern Vizcaino Peninsula (Ophiolite Complex)	Late Triassic	Albian (~105)	MORB	Pillow Basalt	27.016	-113.997	[34]
	Arteaga Complex	Late Triassic (Norian 225 Ma)	Albian (~105)	MORB	Pillow Basalt	18.674	-103.130	[33]

Acc. Comp.	Site	Birth of Oceanic Plate	Age of Accretion	Affinity	Volc. Rock Type	Lat.	Long.	Ref.
	Margarita Magdalena	Late Triassic (Norian 225 Ma)	Albian (~105)	MORB	Pillow Basalt	24.626	-112.143	[33]
California								
Franciscan Complex	Marin Headlands Terrane	Early Jurassic (Pliensbachian ~191 Ma)	Late Cretaceous (Cenomian ~94)	MORB	Pillow Basalt	37.824	-122.498	[25]
	Nicasio Reservoir Terrane	~Early Cretaceous (Berriasian ~140 Ma)	Late Cretaceous (Cenomian ~94)	EMORB	Pillow Basalt	38.079	-122.765	[25, 26, 27]
	Nicasio Reservoir Terrane	~Early Cretaceous (Berriasian ~140 Ma)	Late Cretaceous (Cenomian ~94)	OIB	Gabbro	38.079	-122.765	[25, 26, 27]
	Sunol Regional Wilderness (Yolla Bolly Terrane)	Middle Jurassic (Callovian ~165 Ma)	Late Cretaceous (Cenomian ~100)	MORB	Basaltic protolith (Eclogite)	37.540	-121.811	[25, 26,]
	Pacheco Pass (Dablo Range)	Middle Jurassic (Callovian ~165 Ma)	Early Cretaceous (early Albian ~110 Ma)	MORB	Basalt	36.706	-121.148	[25, 26,]
	Pacfica Quarry (Permanente Terrane)	~Early Cretaceous (Berriasian ~140 Ma)	~Turonian - Coniacian	OIB	Basalt	37.644	-122.493	[25, 26, 28]
	Pacfica (Permanente Terrane)	~Early Cretaceous (Berriasian ~140 Ma)	~Turonian - Coniacian	MORB	Pillow Basalt	37.624	-122.479	[25, 26, 28]
Alaska								
Chugach Terrane	Uyak Bay (Uyak Complex)	~Middle Permian	~Early Cretaceous	E-MORB	Basalt	57.650	-154.044	[21, 22, 54]
	Turnagain Arm (McHugh Complex)	~Middle Trassic (Ladinian)	Late Cretaceous (Aptian-Aptian)	E-MORB	Basalt	60.999	-149.598	[23, 54]
	Kachemak Bay (McHugh Complex)	~Early Jurassic (Toarchian)	Late Cretaceous (Campanian - Maastrichtian)	E-MORB	Basalt	59.445	-151.644	[24, 54]
Phoenix Plates								
New Zealand								
Torlesse Terrane	Esk Head Melange	~Late Triassic	~Early Cretaceous (Aptian 121 Ma)	OIB ???	Pillow Lava	-43.060	172.241	[36, 35]
	Wairarapa Melange	~Late Triassic	~Early Cretaceous (Aptian 121 Ma)	??	Basalt	-41.486	175.581	[50]

Acc. Comp.	Site	Birth of Oceanic Plate	Age of Accretion	Affinity	Volc. Rock Type	Lat.	Long.	Ref.
	Aorangi Range Melange	~Late Triassic	~Early Cretaceous (Aptian 121 Ma)	OIB	Pillow Basalt	-41.588	175.271	[51]
Chrystalls Beach Complex	Watson Beach	~Early Triassic	~Late Triassic (Norian 221 Ma)	MORB	Pillow Basalt	-46.163	170.151	[38]
	Akatore Creek	~Early Triassic	~Late Triassic (Norian 221 Ma)	OIB	Pillow Basalt	-46.115	170.190	[38]
	Taieri Mouth	~Early Triassic	~Late Triassic (Norian 221 Ma)	MORB	Pillow Basalt	-46.188	170.120	[38]
Waipapa Terrane	Whangaroa Bay	Middle Permian ??	Late Triassic (207 Ma)	OIB	Pillow Basalt	-35.002	173.797	[41]
	Arrow Island	Early Triassic	Late Triassic (207 Ma)	OIB	Pillow Basalt (Sills ?)			[41]
	Tawharanui	Early Triassic	Late Jurassic (152 Ma)	MORB, EMORB	Pillow Basalt	-36.371	174.829	[40]
	Whangarei	Early Triassic	Late Jurassic (152 Ma)	MORB, EMORB	Pillow Basalt	-35.839	174.578	[40]
	Kawakawa	Early Triassic	Late Jurassic (152 Ma)	MORB, EMORB	Pillow Basalt	-36.932	175.193	[42]
	Waiheke Island	Early Triassic	Late Jurassic (152 Ma)	MORB, EMORB	Pillow Basalt	-36.783	175.001	[42]

References : [1](Koizumi & Ishiwatari, 2006), [2](Safonova, Kojima, et al., 2015), [3](Ichiyama et al., 2014), [4](S. Sano et al., 2000), [5](H. Sano, 2006), [6](Onoue et al., 2004), [7](Endo & Wallis, 2017), [8](Safonova et al., 2016), [9](Agata, 1994), [10](Nakae, 2000), [11](H. Sano, 1988a), [12](H. Sano, 1988b), [13](Sawada et al., 2019), [14](Ozawa, Murata, Nishimura, et al., 1997), [15](Kimura, 1994), [16](Sakakibara & Ota, 1994), [17](Kimura, 1997), [18](Taira et al., 1988), [19](Ueda & Miyashita, 2005), [20](Kimura et al., 1992), [21](Connelly et al., 1977), [22](Connelly, 1978), [23](Kusky et al., 1997), [24](Kusky & Bradley, 1999), [25](Wakabayashi, 2017), [26](Ghatak et al., 2012), [27](Schnur & Gilbert, 2012), [28](Larue et al., 1989), [29](Baumgartner & Denyer, 2006), [30](Bandini et al., 2011), [31](Boschman et al., 2019), [32](Hauff et al., 2000), [33](Centeno-García et al., 1993), [34](Kimbrough & Moore, 2003), [35](Wandres & Bradshaw, 2005), [36](Wandres et al., 2005), [37](Hada et al., 2006), [38](Fagereng & Cooper, 2010), [39](Yamamoto, 1987), [40](Aita & Spörli, 1992), [41](Takemura et al., 2002), [42](Black, 1994), [43](Zamoras & Matsuoka, 2001), [44](Zamoras & Matsuoka, 2004), [45](Yumul, Dimalanta, Gabo-Ratio, et al., 2020), [46](Queaño, Dimalanta, et al., 2017), [47](Rangin, 1991), [48](Pasco et al., 2019), [49](Tamayo et al., 2001), [50](P. M. Barnes & Korsch, 1991), [51](George, 1993), [52](Tominaga et al., 2019), [53](Tominaga & Hara, 2021), [54](J. M. Amato & Pavlis, 2010)

Table 2. Compilation of Paleomagnetic data of the Upper Paleozoic – Mesozoic Circum Pcific OPS

Location		**Paleomagnetic**							
Lat.	**Long.**	**D**	**ΔDx**	**I**	**ΔIx**	**k**	**α95**	**λ**	**Ref.**
Russia									
47.279	142.967	263.5	52.8	73.4	75.6	<3	50.9		1
47.279	142.967	111.2	156.3	-17.3	-53.3	30	17.9		1
47.279	142.967	210.8	155.2	11.6	51.7	31	17.7		1
47.279	142.967	210.8	164.8	11.6	-51.7	31	17.7		1
47.279	142.967	162.5	160.4	-3.7	-52.6	35	9.6		1
Japan									
35.4	137			1.4	6.8			0.7 ± 3.4	2
35.4	137	252.8		-5.4		126.8	2.3	-2.7	3
35.4	137	48		10.9		26.8	4.4	-5.5	3
35.4	137	339.4		18.2		4.8	26.1	9.3	3
35.4	137	218.7		7.7		6.4	23.4	3.9	3
35.4	137	320.8		20		7.1	53.6	10.3	3
35.4	137	234.2		-7.2		5.5	43.7	3.6	3
35.4	137	154.7		12		3.2	34.3	6.7 ± 17.8	3
35.4	137	-88.8		46.6		9.9	20.2	29.5 ± 17.4	4
35.4	137	111.9		22.6		4.5	25.9	11.8 ± 14.6	4
35.4	137	82.4		39.4		8.1	19.3	23.5 ± 14.2	4
35.4	137	132.7		16.5		2.9	43.3	9 ± 23.3	4
35.4	137	94.5		29.4		12.5	16.3	16.9 ± 10.2	4
32.8	131.3	327.5		-23.4		13.99	3.2	-12.2 ± 1.8	5
42.674	142.674	251.4	8	7.2	15.7	9.7	10	3.6	6
Costa Rica									
10.879	-85.875	45.7	4.3	24.9	7.3	22.1	4.3	13	6
10.881	-85.879	350.1	9.5	-15.7	17.8	19.9	10	8	6

Location		Paleomagnetic							
Lat.	**Long.**	**D**	**ΔDx**	**I**	**ΔIx**	**k**	**α95**	**λ**	**Ref.**
10.815	-85.733	213.8	3.6	36.6	5	41.7	3.9	20.4	[6]
Mexico									
28.056	-115.227	208.8	11.2	5.5	22.3	16.3	12.3	2.7	[6-7]
28.114	-115.275	189.4	7	-10	13.6	17.1	7.7	5	[6]
California									
38	237.3	145.3		-52.9		23	7.3		[8]
40.3	235.8	78		47		11	9.2		[9]
37.8	237.5	113.2		46.8		8.2	16		[10]
42.4	236.1	124		37		12	11.2		[11]
New Zealand									
-35.250	174.133	19.2	13.1	23.9	22.4	6.1	16.9	12.5	[6]
-35.250	174.133	165.3	13	-27.3	21.1	11.3	15	14.5	[6]
-35.257	174.133	320.4	9.7	14	18.4	55.6	10.3	7.1	[6]
-38.6	174.9	349		-53		5	17	-33.6	[12]

References : [1](Bazhenov et al., 2001), [2](Shibuya & Sasajima, 1986b), [3](Ando et al., 2001), [4](Oda & Suzuki, 2000), [5](Kirschvink et al., 2015), [6](Boschman et al., 2021), [7](Hagstrum & Sedlock, 1992), [8](Harbert et al., 1984), [9](Gromme & Gluskoter, 1965), [10](Curry et al., 1984), [11](Blake Jr et al., 1985), [12] (Kodama et al., 2007).